宇宙物理学と状態方程式

京都大学大学院理学研究科
中村卓史

2005年12月26日理論懇シンポ

例１） 球対称な星の進化

状態方程式は基本的に良く判っている

圧力＝輻射圧＋ガス圧＋縮退圧

核反応も主要なものは良く判っている

対流によるエネルギー輸送＝？だったが太陽ニュートリノでOK?

輻射の輸送、輻射の物質による散乱吸収再放出等も主要な部分は良く判っている

結論として基礎方程式と数値解法が確立している、

その結果著者にあまりよらない結果が得られていて教科書に書かれている

例2） 回転していたり質量放出する星の進化

状態方程式は例１）と同じ

角運動量の輸送の理論の基礎方程式や

質量放出の基礎方程式がはっきりしていないので

教科書に書くレベルには至っていない。

例3） 宇宙

圧力＝輻射圧＋ダークエネルギーの負の圧力

ダークエネルギーの理論はない！！

観測が先に進んでいるが、独立な検証が必要！！

種々の方法の適用と提案

1） Typela 超新星、

2） WMAP,

3） Baryon Acoustic Oscilation

4） GRBの光度ーピークエネルギー関係

5) 合体1年前の連星中性子星

The Supernova Legacy Survey: Measurement of Ω_M, Ω_Λ and w from the First Year Data Set ⋆

arXiv:astro-ph/0510447 v1 14 Oct 2005

fit	parameters (stat only)
$(\Omega_M, \Omega_\Lambda)$	$(0.31 \pm 0.21, 0.80 \pm 0.31)$
$(\Omega_M - \Omega_\Lambda, \Omega_M + \Omega_\Lambda)$	$(-0.49 \pm 0.12, 1.11 \pm 0.52)$
$(\Omega_M, \Omega_\Lambda)$ flat	$\Omega_M = 0.263 \pm 0.037$
$(\Omega_M, \Omega_\Lambda)$ + BAO	$(0.271 \pm 0.020, 0.751 \pm 0.082)$
(Ω_M, w)+BAO	$(0.271 \pm 0.021, -1.023 \pm 0.087)$

Table 3 Cosmological parameters and statistical errors of Hubble diagram fits, with the BAO prior where applicable.

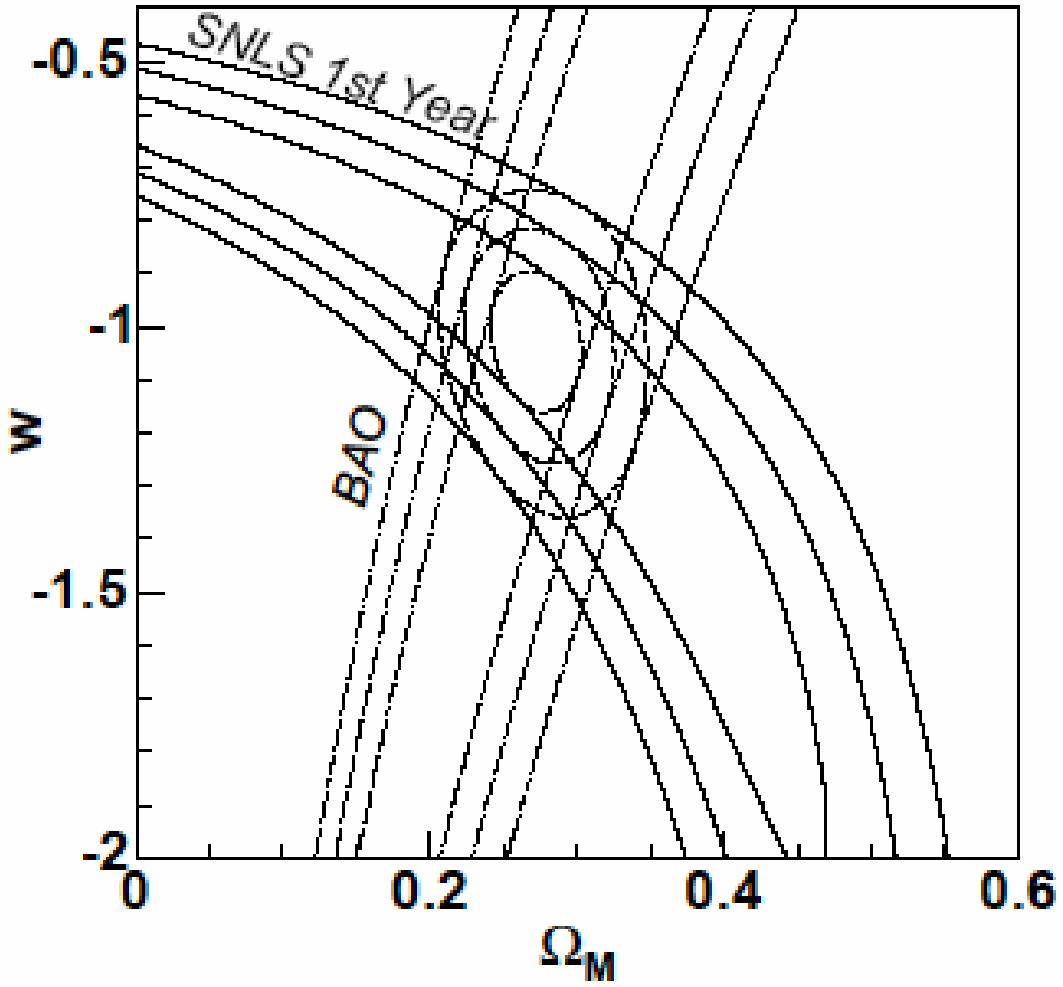

Fig. 6 Contours at 68.3%, 95.5% and 99.7% confidence levels for the fit to a flat (Ω_M, w) cosmology, from the SNLS Hubble diagram alone, from the SDSS baryon acoustic oscillations alone (Eisenstein et al. 2005), and the joint confidence contours.

中性子星の発見

ベルが最初に見た電波パルサー　　P=1.3373011秒

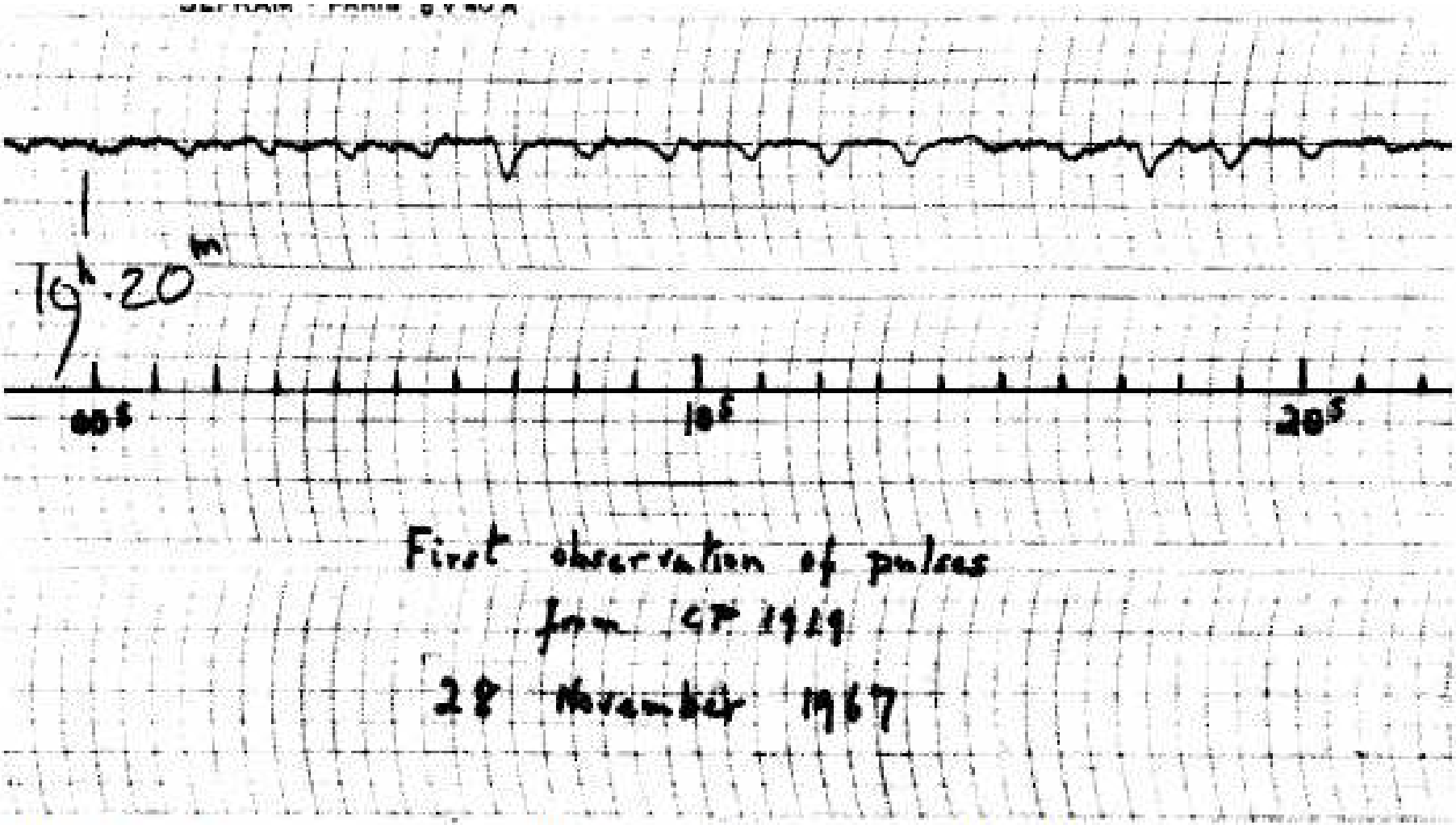

Fig. 2. The first indication of pulsed radio emission from CP 1919.

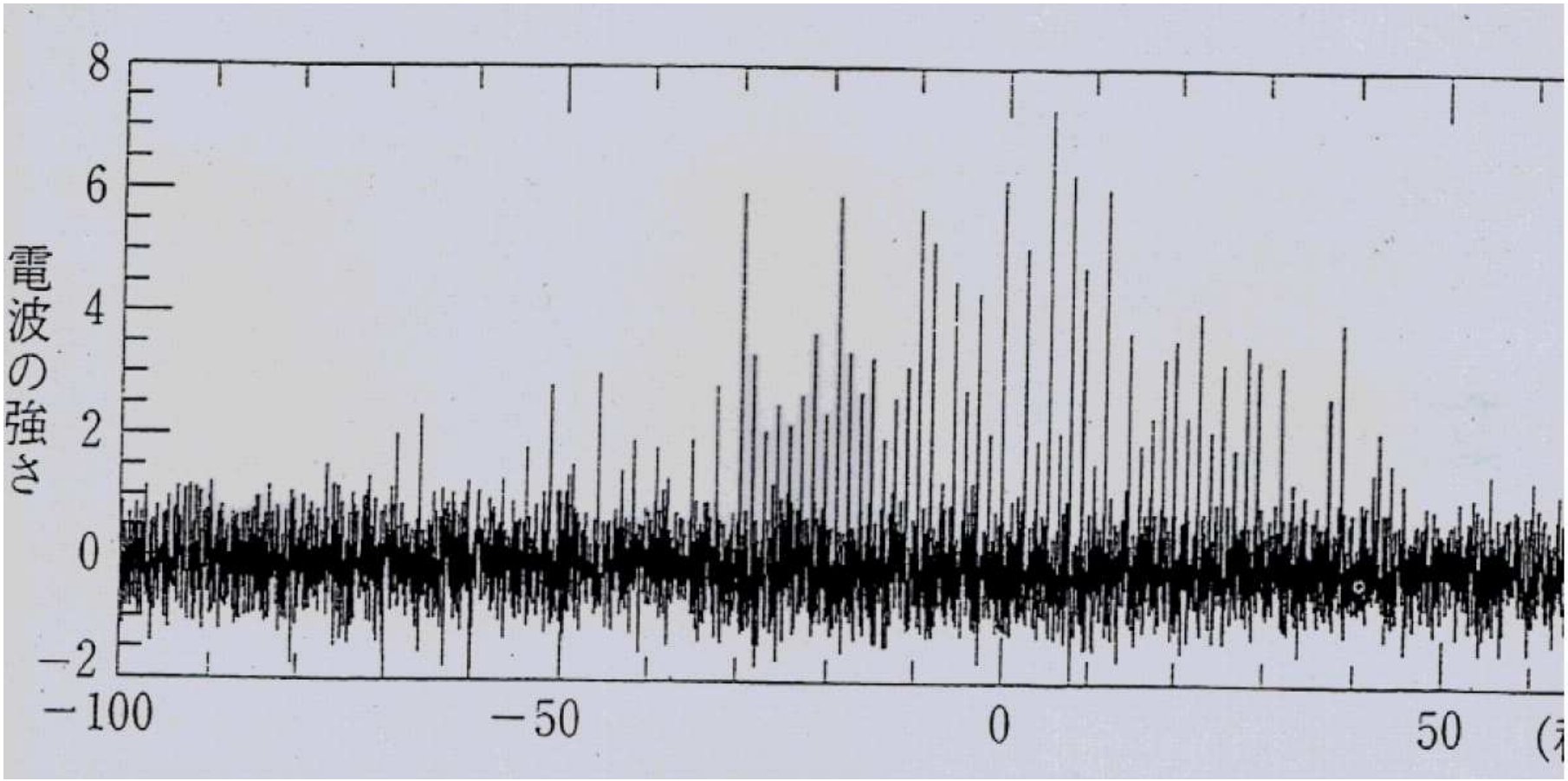

観測時間（秒）

現在約1700個　周期は1．4msから　数秒

- 重力が遠心力以上でないと、天体はバラバラになってしまう。
- 未知の天体の質量をM、半径をRとしてみよう

$$\frac{GM}{R^2} > R\Omega^2 \rightarrow \bar{\rho} > \frac{3\Omega^2}{4\pi G}$$

$$\Omega = \frac{2\pi}{1.4\mathrm{ms}} \rightarrow \bar{\rho} > 7.1 \times 10^{13}\mathrm{gcm}^{-3}$$

- 原子核の密度　$\sim 3 \times 10^{14}\mathrm{gcm}^{-3}$
- 星を作っている普通の物質
  陽子:中性子:電子＝1:1:1
- 普通の密度では電子は原子核のはるか外にあるが、このような高密度では電子と陽子が接するので電子捕獲が進んで中性子過剰物質となる。

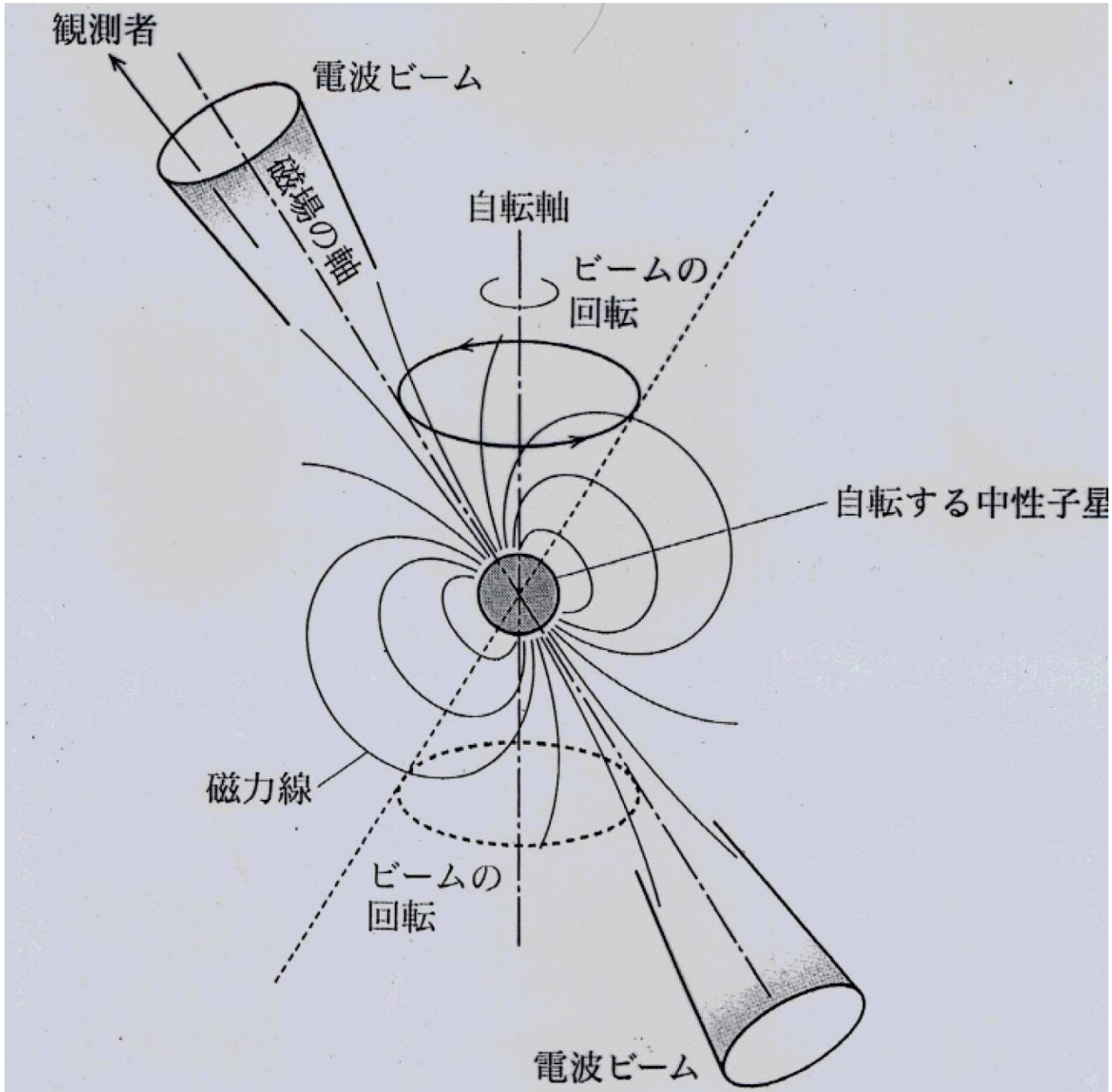

図2　パルサーの模式図．自転している中性子星で，磁場の軸の向きが自転軸と異なると，磁場の軸の方向に電波ビームが放出されると考えられている．

Binary and Millisecond Pulsars

Duncan R. Lorimer

arXiv:astro-ph/0511258 v1 9 Nov 2005

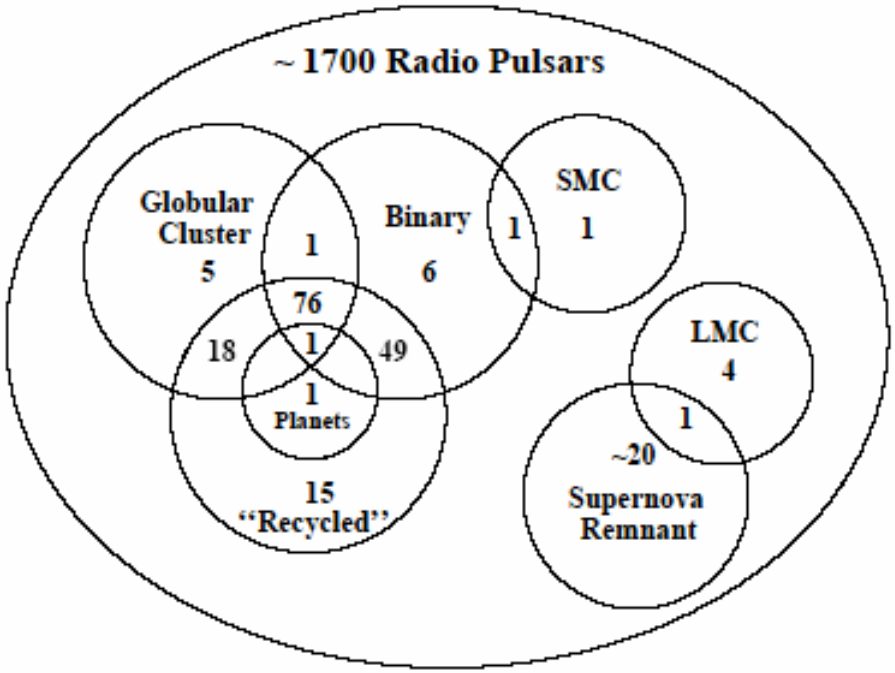

Figure 1: *Venn diagram showing the numbers and locations of the various types of radio pulsars known as of January 2005. The large and small Magellanic clouds are denoted by LMC and SMC.*

dP/dt

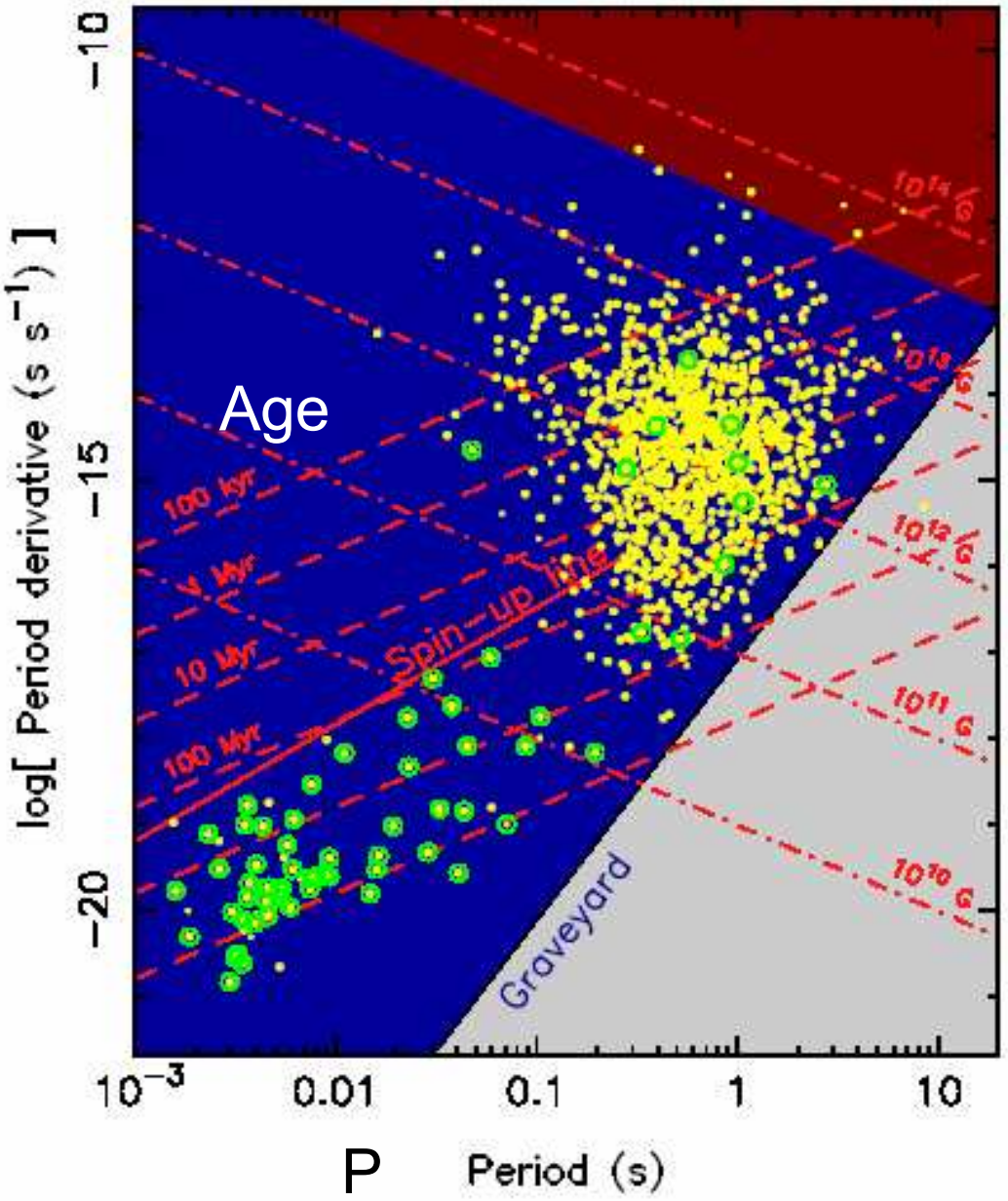

B

Binary

Figure 3: *The P–Ṗ diagram showing the current sample of radio pulsars. Binary pulsars are highlighted by open circles. Theoretical models [64] do not predict radio emission outside the dark blue region. Figure provided by Michael Kramer.*

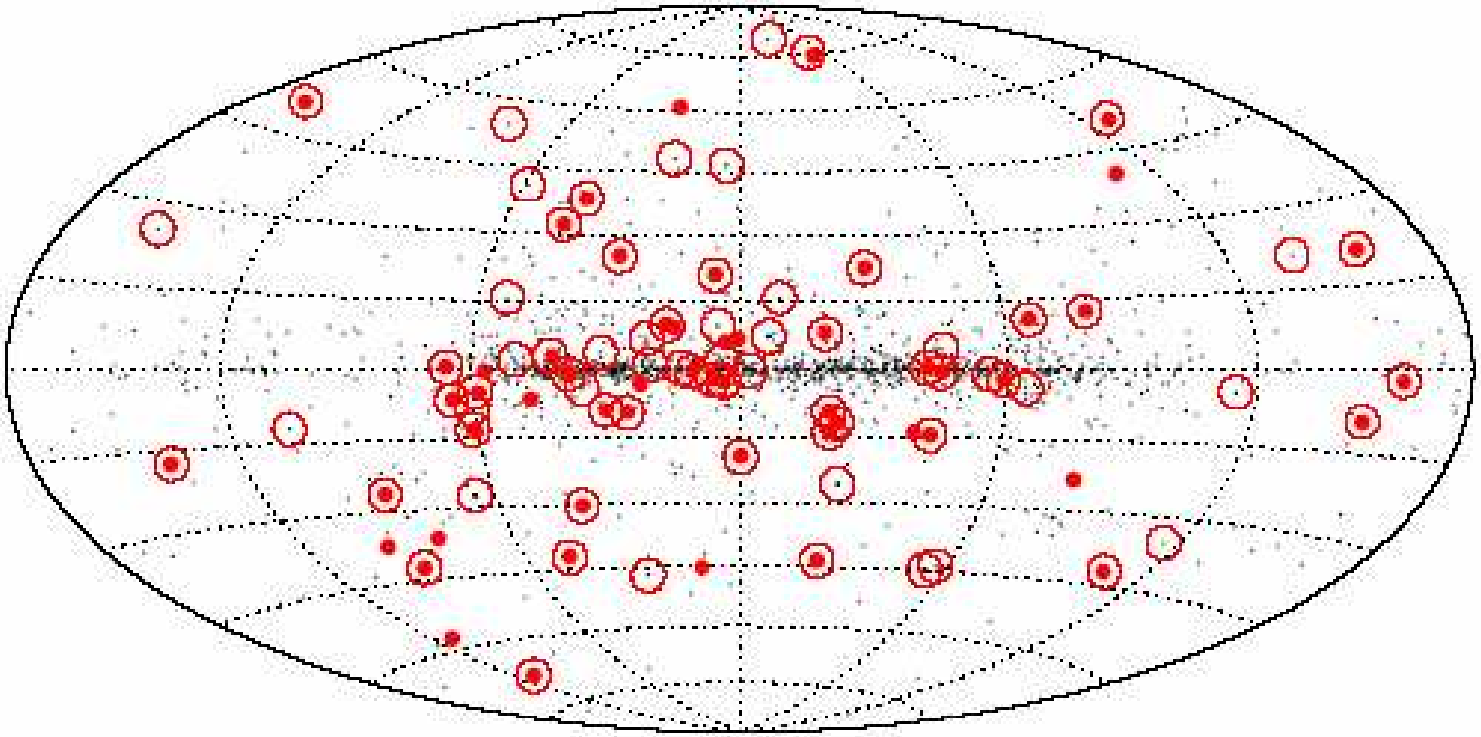

Figure 6: *The sky distribution of pulsars in Galactic coordinates. The plane of the Galaxy is the central horizontal line. The Galactic centre is the midpoint of this line. Millisecond pulsars are indicated in red. Binary pulsars are highlighted by the open circles. The more isotropic distribution of the millisecond and binary pulsars reflects the differences in detecting them out to large distances cf. the normal population (see Section 3).*

● Millisecond Pulsar ○ Binary

Spiral structure

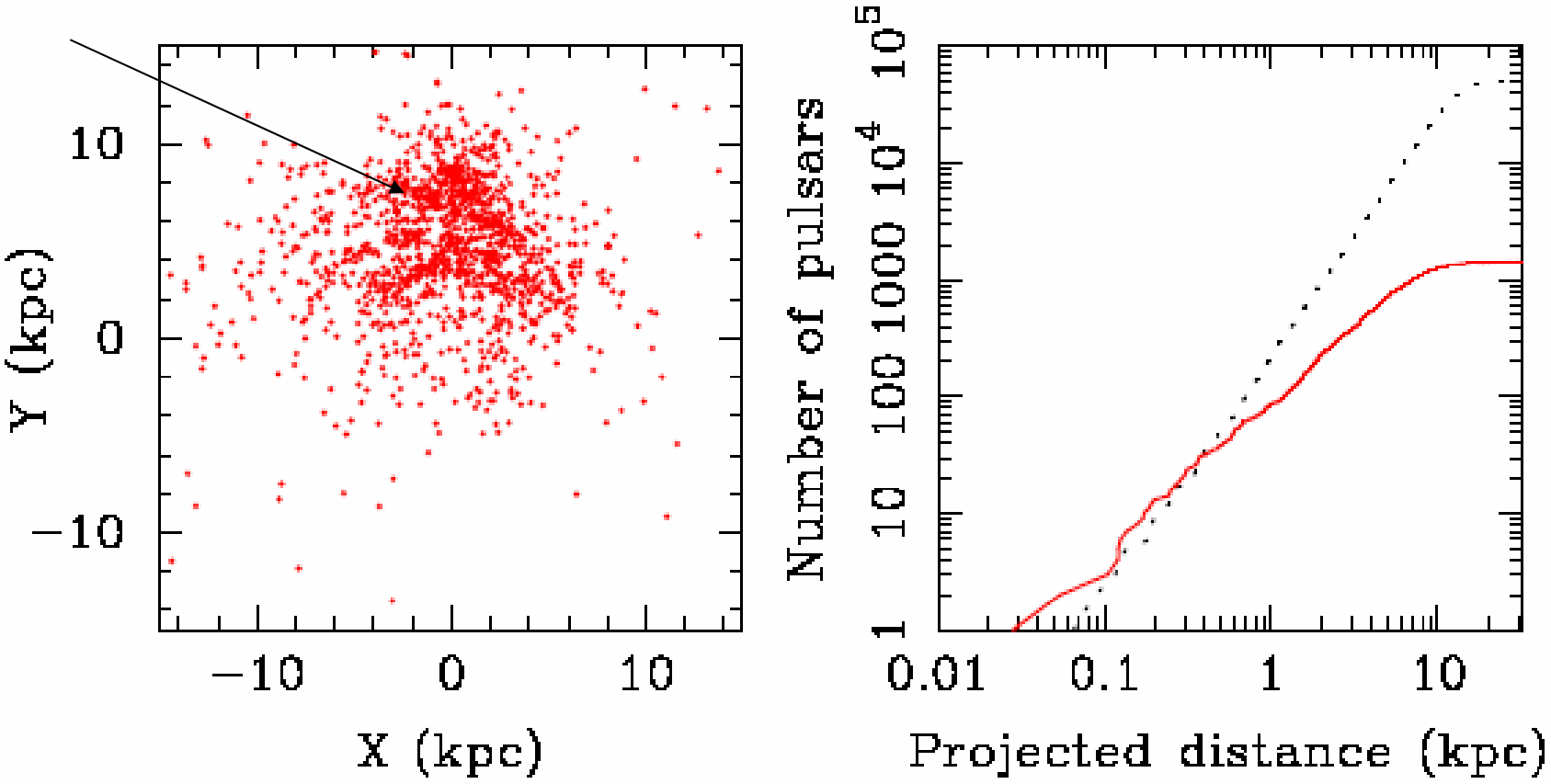

Figure 11: *Left panel: The current sample of all known radio pulsars projected onto the Galactic plane. The Galactic centre is at the origin and the Sun is at* $(0, 8.5)$ kpc. *Note the spiral-arm structure seen in the distribution which is now required by the electron density model [73, 74]. Right panel: Cumulative number of pulsars as a function of projected distance from the Sun. The solid line shows the observed sample while the dotted line shows a model population free from selection effects.*

TOV方程式

- 一般相対論的平衡解(Tolman Oppenheimer Volkov 方程式)

$$\frac{dp}{dr} = -\rho \frac{Gm}{r^2} f$$

f >1

$$f = (1 + \frac{4\pi r^3 p}{mc^2})(1 + \frac{p}{\rho c^2})(1 - \frac{2Gm}{rc^2})^{-1}$$

$$p = p(\rho)$$

太陽質量単位で測った中性子星の質量

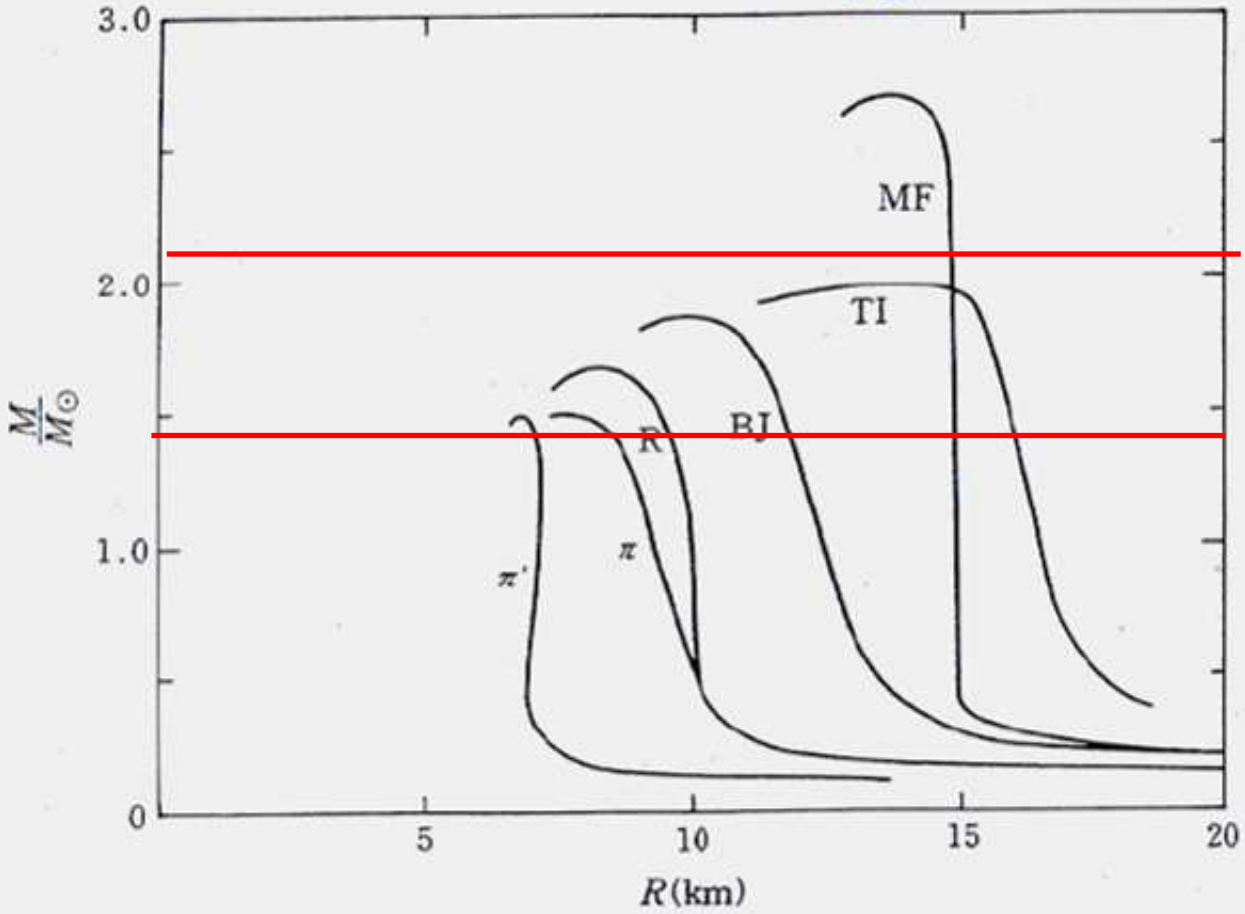

2.1

1.44

図 3-4　中性子星の半径と質量の関係．質量が小さくなると半径が増大することに注意．[Baym and Pethick 1979]

どの状態方程式が正しいのか全く不明

中性子星の最大質量

- TOV方程式が正しい
- 物質の音速は光速以下である。(因果律)
- 核密度以下での状態方程式を知っている。
- 中性子星の最大質量は

$3.2M_\odot$ Rhoades&Ruffini 1974

$M > 3.2M_\odot$ 重力平衡解はない

1)ブラックホールの存在証明に状態方程式の詳細は不要
2)観測された中性子星の質量より最大質量が
小さい状態方程式はダメである。

ブラックホール候補X線星

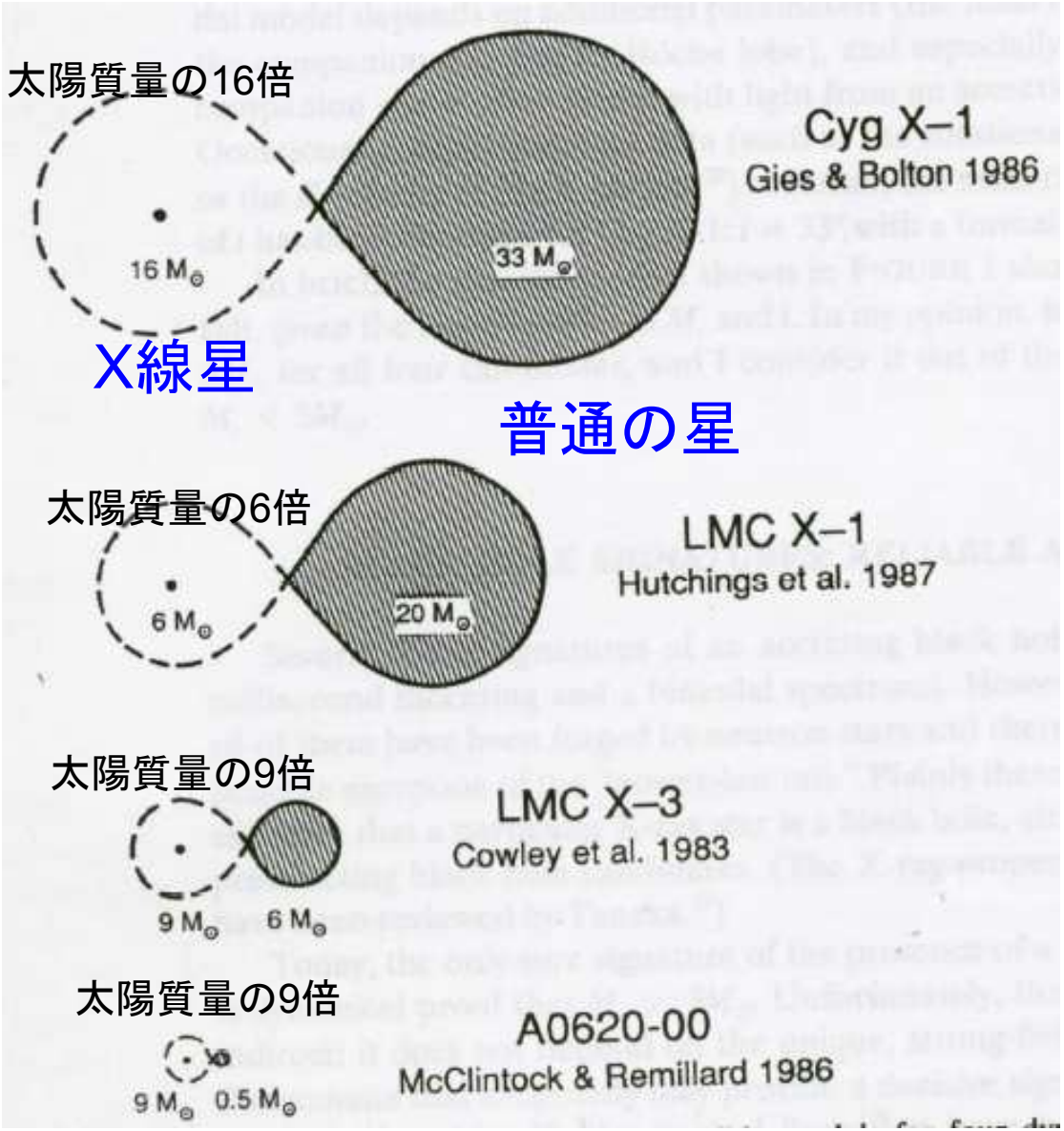

18個のブラックホール候補天体

Table 4.2. *Confirmed black hole binaries: X-ray and optical data*

Source	f(M)[a] ($M_\odot$)	M_1^a ($M_\odot$)	f(HFQPO) (Hz)	f(LFQPO) (Hz)	Radio[b]	E^c_{max} (MeV)	References
0422+32	1.19±0.02	3.2–13.2	–	0.035–32	P	0.8,1–2:	1,2,3,4,5
0538–641	2.3±0.3	5.9–9.2	–	0.46	–	0.05	6,7
0540–697	0.14±0.05	4.0–10.0:	–	0.075	–	0.02	8,7
0620–003	2.72±0.06	8.7–12.9	–	–	P,J?	0.03:	9,10,11
1009–45	3.17±0.12	6.3–8.0	–	0.04–0.3	–[d]	0.40, 1:	12,4,13
1118+480	6.1±0.3	6.5–7.2	–	0.07–0.15	P	0.15	14,15,16,17
1124–684	3.01±0.15	6.5–8.2	–	3.0-8.4	P	0.50	18,19,20,21
1543–475	0.25±0.01	7.4–11.4[e]	–	7	–[f]	0.20	22,4
1550–564	6.86±0.71	8.4–10.8	92,184,276	0.1-10	P,J	0.20	23,24,25,26,27
1655–40	2.73±0.09	6.0–6.6	300,450	0.1–28	P,J	0.80	28,29,30,31,54
1659–487	> 2.0[g]	–	–	0.09–7.4	P	0.45, 1:	32,33,4,13
1705–250	4.86±0.13	5.6–8.3	–	–	–[d]	0.1	34,35
1819.3–2525	3.13±0.13	6.8–7.4	–	–	P,J	0.02	36,37
1859+226	7.4±1.1	7.6–12:	190	0.5–10	P,J?	0.2	38,39,40,41
1915+105	9.5±3.0	10.0–18.0:	41,67,113,168	0.001-10	P,J	0.5, 1:	42,43,44,4,13
1956+350	0.244±0.005	6.9–13.2	–	0.035–12	P,J	2–5	45,46,47,48,49
2000+251	5.01±0.12	7.1–7.8	–	2.4–2.6	P	0.3	18,50,51
2023+338	6.08±0.06	10.1–13.4	–	–	P	0.4	52,53

中性子星の質量の観測

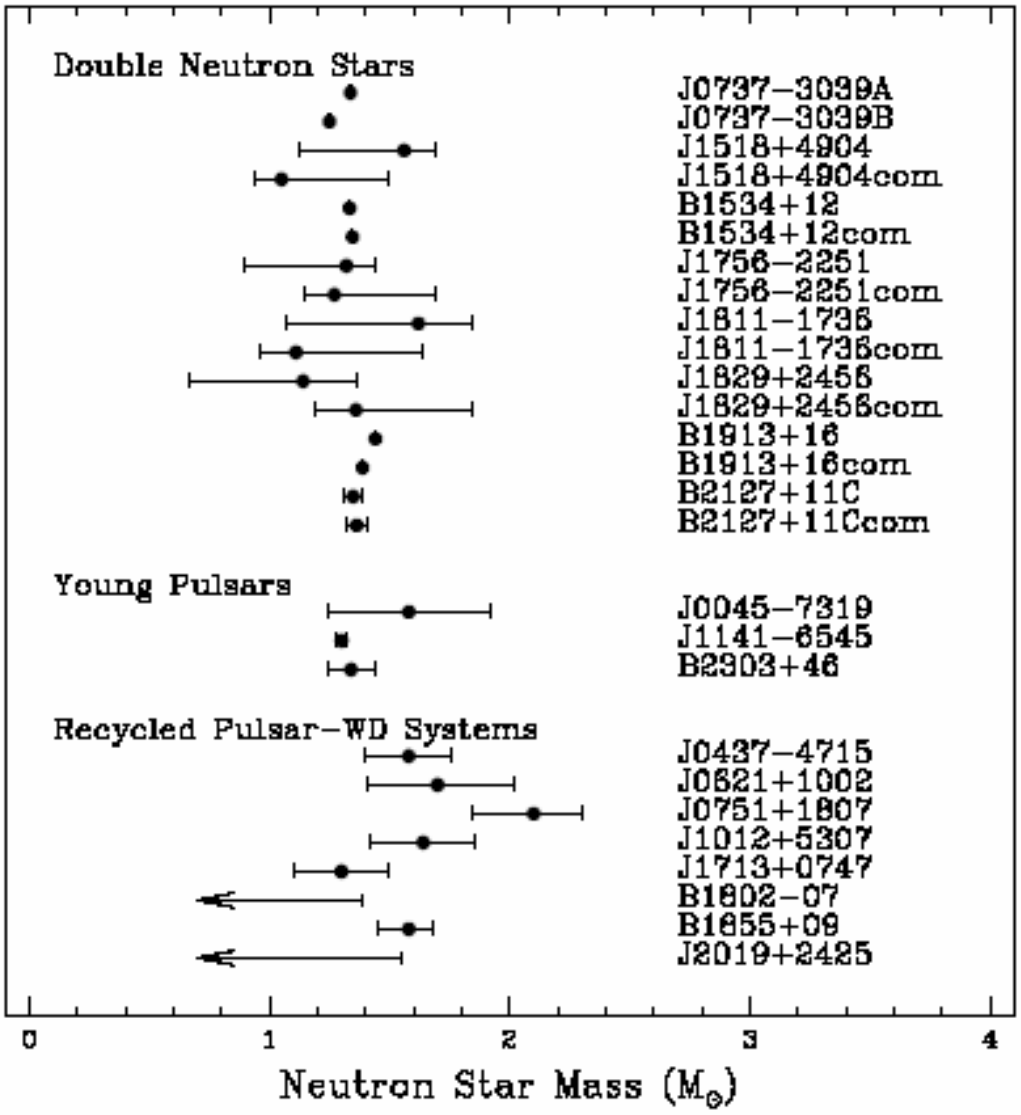

Figure 28: *Distribution of neutron star masses as inferred from timing observations of binary pulsars [292]. The vertical dotted line shows the canonical neutron star mass of* $1.4\,M_{\odot}$. *Figure provided by Ingrid Stairs.*

中性子星の質量が4桁の精度で決まった連星パルサーPSR1913＋16（1993年度ノーベル物理学賞）

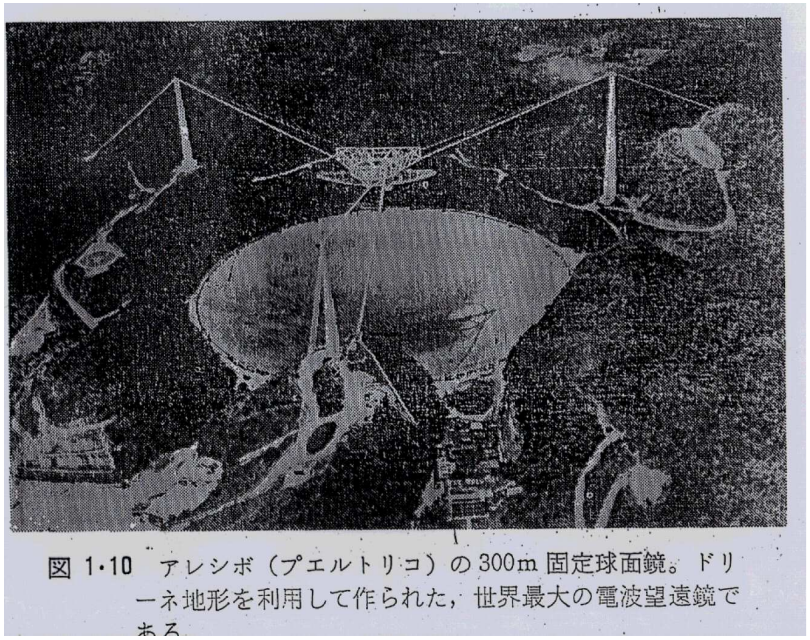

図 1·10　アレシボ（プエルトリコ）の 300m 固定球面鏡。ドリーネ地形を利用して作られた，世界最大の電波望遠鏡である

連星の軌道パラメター

- 軌道長半径　～　７０万km（ほぼ太陽の半径）
- 公転周期　　～　８時間
- 楕円　（離心率　～　０．６）

- 電波パルサー　＝　正確な時計
- 例　PSR1937＋21のパルス周期
  １．５５７８０６４６８１９７９４ミリ秒
- 連星パルサー　PSR1913＋16は自然が与えてくれた「一般相対論の実験場」

- 約15年間のPSR1913＋16からの電波パルスの到着時間のデータ解析から

表 3-2　PSR1913+16 の位置パラメータ

α	$19^h15^m28^s.00018(15)$
δ	$16°06'27''.4043(3)$
μ_α (10^{-3} arcsec yr^{-1})	-3.2 ± 1.8
μ_δ (10^{-3} arcsec yr^{-1})	1.2 ± 2.0
ν (s^{-1})	16.940539303295(2)
$\dot{\nu}$ (10^{-15} s^{-2})	$-2.47583(2)$
$\ddot{\nu}$ (10^{-27} s^{-3})	< 6

e	$=$	0.6171308(6)
$\dot{\omega}$	$=$	4.226621(6) deg yr^{-1}
γ	$=$	4.295(2) ms
P_b	$=$	27906.9807804(6) s
$\dot{P}_b$	$=$	$-2.425(2)10^{-12}$ s s^{-1}

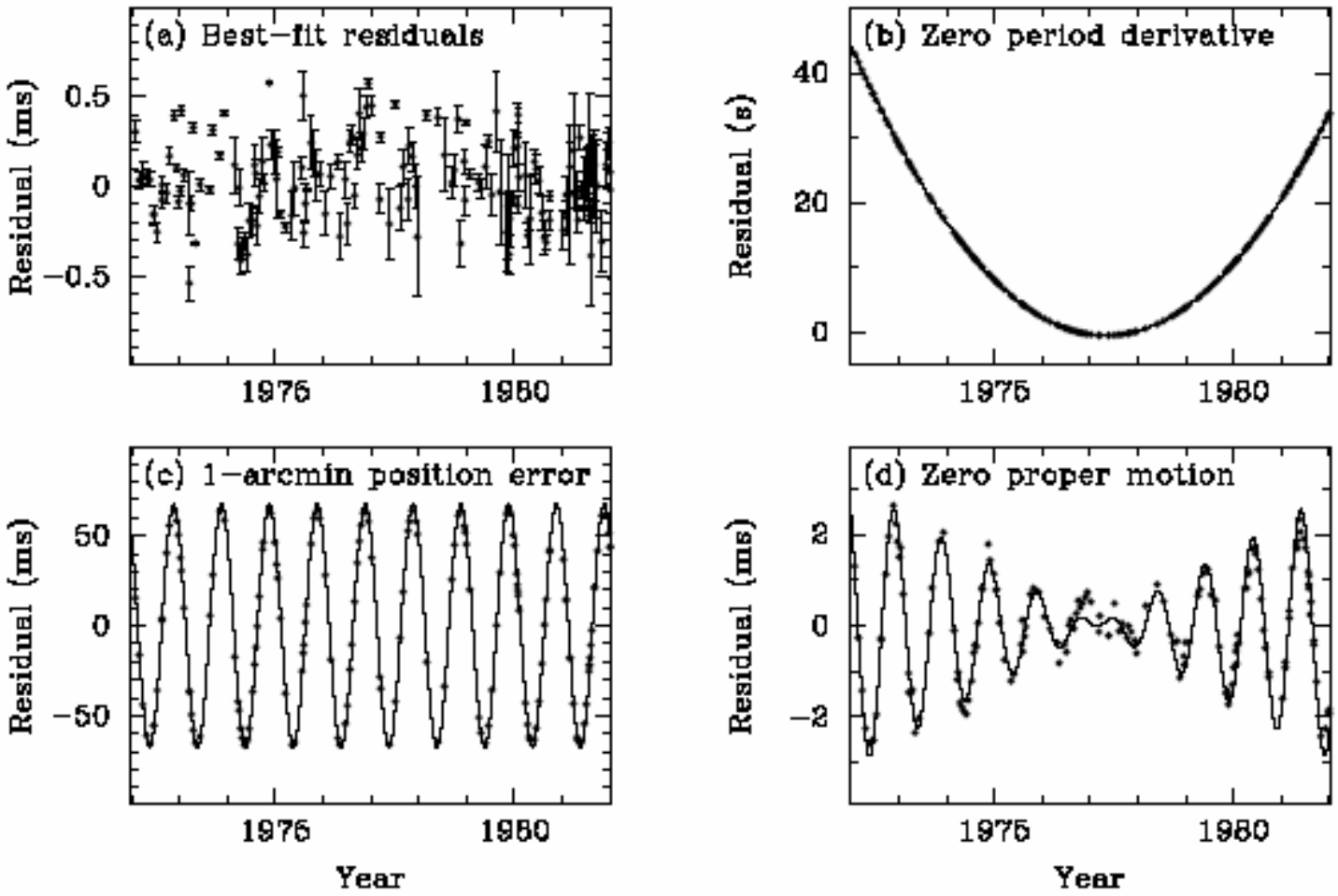

Figure 22: *Timing model residuals for PSR B1133+16. Panel a: Residuals obtained from the best-fitting model which includes period, period derivative, position and proper motion. Panel b: Residuals obtained when the period derivative term is set to zero. Panel c: Residuals showing the effect of a* 1-arcmin *position error. Panel d: Residuals obtained neglecting the proper motion. The lines in Panels b–d show the expected behaviour in the timing residuals for each effect. Data provided by Andrew Lyne.*

$$\dot{\omega} = 3\left(\frac{P_b}{2\pi}\right)^{-5/3} (T_\odot M)^{2/3} (1-e^2)^{-1},$$

$$\gamma = e\left(\frac{P_b}{2\pi}\right)^{1/3} T_\odot^{2/3} M^{-4/3} m_2 (m_1 + 2m_2),$$

$$\dot{P}_b = -\frac{192\pi}{5}\left(\frac{P_b}{2\pi}\right)^{-5/3}\left(1+\frac{73}{24}e^2+\frac{37}{96}e\right)(1-e^2)^{-7/2} T_\odot^{5/3} m_1 m_2 M^{-1/3},$$

$$r = T_\odot m_2,$$

$$s = x\left(\frac{P_b}{2\pi}\right)^{-2/3} T_\odot^{-1/3} M^{2/3} m_2^{-1}.$$

$$r = \frac{Gm_2}{c^3} \quad s = \sin i$$

$$x = a_1 \sin i$$

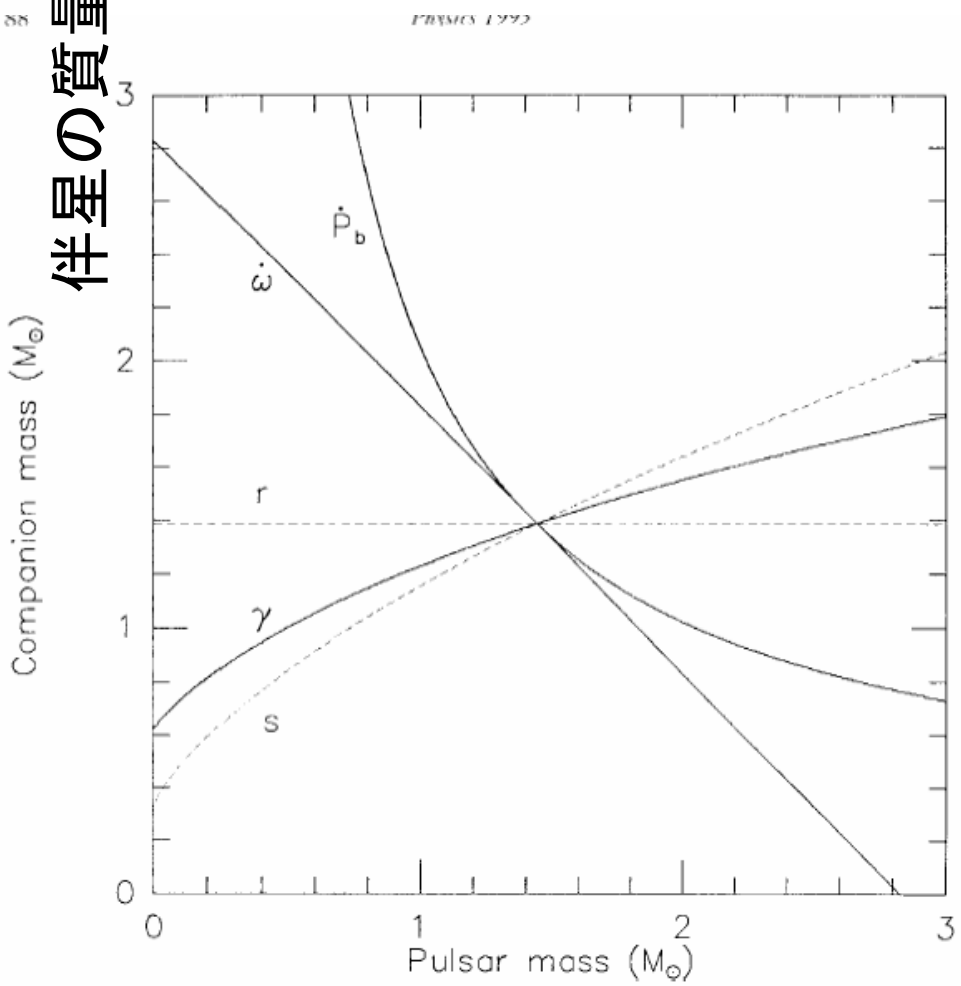

主星の質量

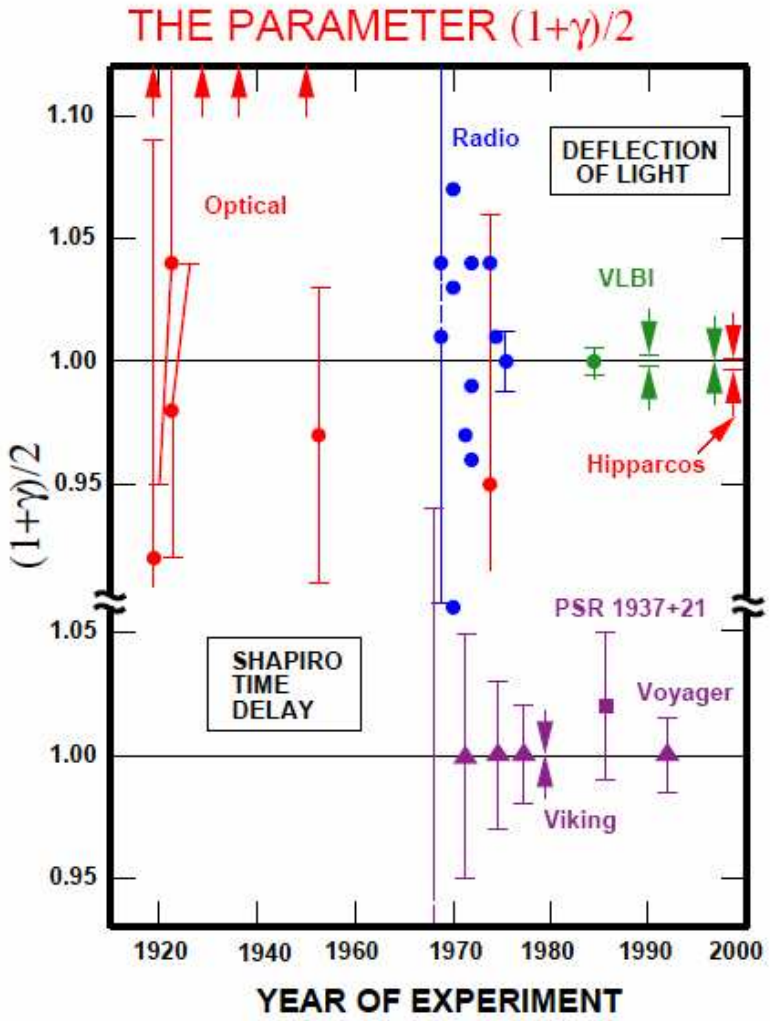

Figure 5: Measurements of the coefficient $(1+\gamma)/2$ from light deflection and time delay measurements. General relativity value is unity. Arrows denote anomalously large values from early eclipse expeditions. Shapiro time-delay measurements using Viking spacecraft yielded agreement with GR to 0.1 percent, and VLBI light deflection measurements have reached 0.02 percent. Hipparcos denotes the optical astrometry satellite, which has reached 0.1 percent.

40

The Confrontation between General Relativity and Experiment

Clifford M. Will

gr-qc/0103036 v1 12 Mar 2001

光の曲がりは0．02%の精度で確認されている。（Will 2001）

シャピロ時間遅れは0．1%の精度で確認されている。

Shapiro Time delay

$$\Delta t = \frac{4GM}{c^3} \ln \frac{4 r_E r_p}{d^2}$$

$$r_E \gg d, r_p \gg d$$

$$\frac{4GM_\odot}{c^3} = 20 \mu s$$

Binary Pulsar Case

$$\Delta t = -2 \frac{G m_2}{c^3} \ln \left(\frac{1 + e \cos \phi}{1 - \sin i \sin(\omega + \phi)} \right)$$

r

s

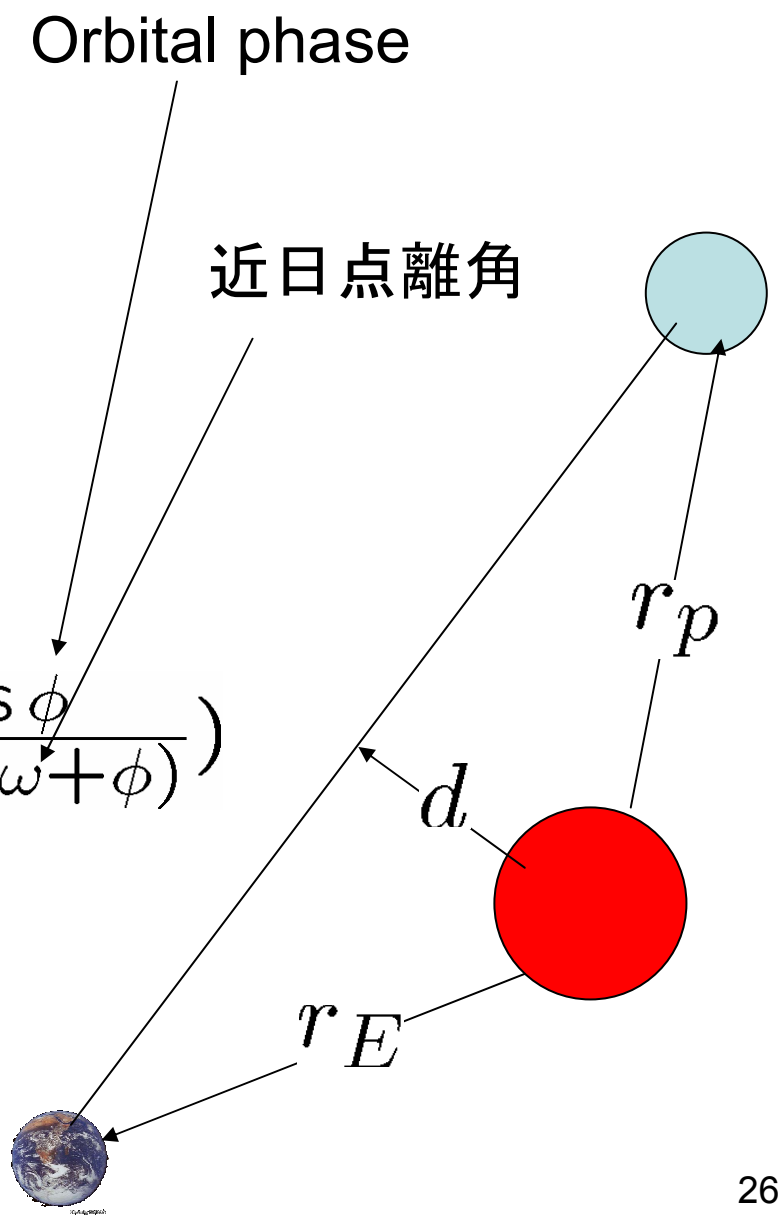

両中性子星の質量が正確に決まった

- $m_1 = 1.4411(7)$ 太陽質量
- $m_2 = 1.3874(7)$ 太陽質量

- それ以外の大発見として、公転周期が1年間に　76．94マイクロ秒短くなっていることが分かった。
- これは、何を意味するのか？⇒重力波の存在の間接的な証明
- ケプラーの法則によると公転周期の2乗は軌道長半径の3乗に比例するので、両中性子星が近づいていることになる。

- PSR1913＋16は連星系なので加速度運動をしている。⇒重力波が放射されている。⇒重力波は正のエネルギーを持っているので連星系はエネルギーを失う。⇒連星は近づく⇒周期は短くなる
- アインシュタインの一般相対性理論による理論計算によると1年間に76．15マイクロ秒公転周期が短くなるはずである。
- 先に得られた観測値との誤差はわずかに0.1%程度である。

しかし、重力波が直接観測されたわけではない。

発見された連星中性子星のリスト

Table 2. Binary systems containing radio pulsars which coalesce in less than 10^{10} yr.

PSR	P (ms)	P_b (hr)	e	Total Mass $M_\odot$	τ_c (Myr)	τ_{GW} (Myr)	Reference
J0737−3039A	22.70	2.45	0.088	2.58	210	87	Burgay et al. (2003)
J0737−3039B	2773	2.45	0.088	2.58	50	87	Lyne et al. (2004)
B1534+12	37.90	10.10	0.274	2.75	248	2690	Wolszczan (1990)
J1756−2251	28.46	7.67	0.181	2.57	444	1690	This Letter 2004
B1913+16	59.03	7.75	0.617	2.83	108	310	Hulse & Taylor (1975)
B2127+11C	30.53	8.04	0.681	2.71	969	220	Anderson et al. (1990
J1141−6545†	393.90	4.74	0.172	2.30	1.4	590	Kaspi et al. (2000)
J1906+0746	144	4	0.085	2.6	0.144	300	

Note. — One neutron star–white dwarf† and 5 DNS systems. PSR B2127+11C is in a globular cluster implying a different formation history to the Galactic DNS systems. Here, τ_c is the pulsars' characteristic age and τ_{GW} is the time remaining to coalesce due to emission of gravitational radiation. The total coalescence time is $\tau_c + \tau_{GW}$.

Table 1. Observed and derived parameters of PSR J1906+0746.

Parameter	Value
Right ascension (J2000)	$19^{h}06^{m}48^{s}.673(6)$
Declination (J2000)	$07°46'28.6(3)''$
Spin period, P (ms)	144.071929982(3)
Spin period derivative, $\dot{P}$	$2.0280(2) \times 10^{-14}$
Epoch (MJD)	53590
Orbital period, P_b (days)	0.165993045(8)
Projected semi-major axis, x (lt s)	1.420198(2)
Orbital eccentricity, e	0.085303(2)
Epoch of periastron, T_0 (MJD)	53553.9126685(6)
Longitude of periastron, ω (deg)	61.053(1)
Periastron advance rate, $\dot{\omega}$ ($^\circ$ yr^{-1})	7.57(3)
Dispersion measure, DM (cm^{-3} pc)	217.780(2)
Rotation measure, RM (rad m^{-2})	+150(10)
Flux density at 0.4 GHz, $S_{0.4}$ (mJy)	0.9(2)
Flux density at 0.8 GHz, $S_{0.8}$ (mJy)	0.72(15)
Flux density at 1.4 GHz, $S_{1.4}$ (mJy)	0.55(15)
Flux density at 3.2 GHz, $S_{3.2}$ (mJy)	0.12(3)
Flux density at 6.0 GHz, $S_{6.0}$ (mJy)	0.030(7)
Main pulse widths at 50 and 10% (ms)	0.6 and 1.7
Characteristic age, $\tau_c = P/2\dot{P}$ (kyr)	112
Magnetic field, $B = 3.2 \times 10^{19}(P\dot{P})^{1/2}$ (Gauss)	1.7×10^{12}
Spin-down power, $\dot{E} = 3.95 \times 10^{46}\dot{P}/P^3$ (ergs s^{-1})	2.7×10^{35}
Inferred distance, d (kpc)	~ 5.4
Spectral index, α	–1.3(2)
Radio luminosity at 1.4 GHz, $S_{1.4}d^2$ (mJy kpc^2)	~ 16
Mass function, $f(m_p, m_c) = 4\pi^2 x^3/(\mathrm{T}_\odot P_b^2)$ ($M_\odot$)	0.1116222(6)
Total system mass, $M = m_p + m_c$, ($M_\odot$)	2.61(2)
Gravitational wave coalescence time, τ_g (Myr)	~ 300

PSR J1906+0746-like objects to be $\sim 60 \times (0.2/f)$ Myr^{-1},

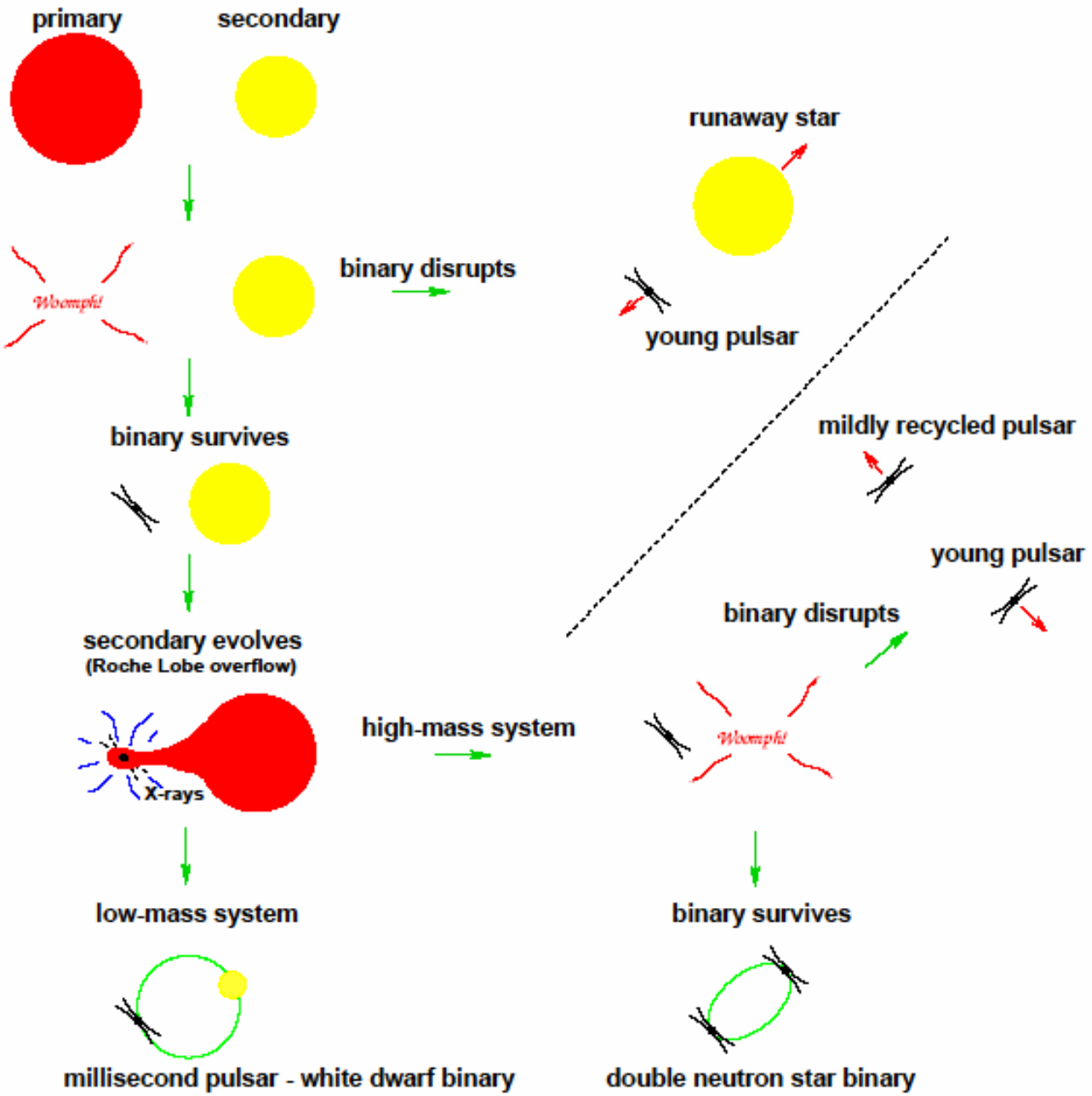

Figure 7: *Cartoon showing various evolutionary scenarios involving binary pulsars.*

中性子星と白色矮星の連星

質量降着時期があるので中性子星の質量が増大する可能性あり。

Heavy Neutron Stars? A Status Report on Arecibo Timing of Four Pulsar–White Dwarf Systems

David J. Nice & Eric M. Splaver

Physics Department, Princeton University
Box 708, Princeton, NJ 08544 USA

Ingrid H. Stairs

Department of Physics and Astronomy, University of British Columbia
6224 Agricultural Road, Vancouver, BC V6T 1Z1, Canada

arXiv:astro-ph/0311296 v1 12 Nov 2003

Keplerの第3法則から $f_1 = (m_2 \sin i)^3 (m_1 + m_2)^{-2}$:

3つの変数に1つの関係のみ $m_1,\ m_2,\ \sin i$

これ以外に、1） 近日点移動 2）シャピロタイムディレー
3）重力波放出による公転周期の減少の
2つが必要

Table 1. Mass Measurements from Timing Analysis

Pulsar	Orbital Period P_b (days)	Eccentricity e	Mass Function f_1 ($M_\odot$)	Pulsar Mass (95% confidence) m_1 ($M_\odot$)
J 0621+1002	8.32	0.002 457	0.0270	1.1–2.3
J 0751+1807	0.26	0.000 003	0.0010	1.6–2.8
J 1713+0747	67.83	0.000 075	0.0079	1.2–2.1
B1855+09	12.33	0.000 022	0.0056	1.4–1.8

軌道周期の減少とSin i

近日点移動
Mch以下

Sin i
進化理論

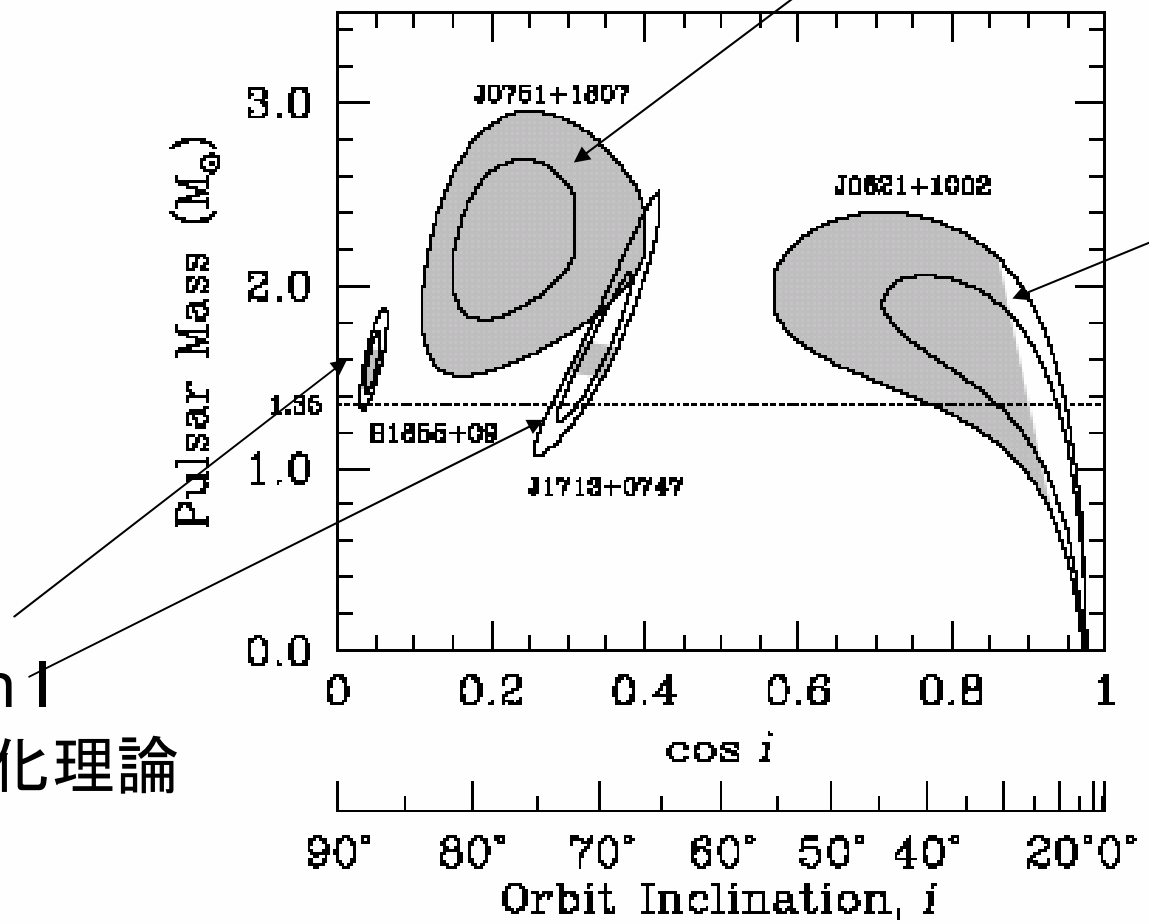

Figure 1. Constraints on pulsar masses and orbital inclinations. Inner and outer contours are 68% and 95% confidence regions, respectively, based on timing data alone. Shaded areas indicate theoretical limits within these contours, from the assumption that the companion is a white dwarf (J0621+1002) and from predictions of secondary star masses from the $P_b - m_2$ relation (B1855+09 and J1713+0747). (There are no theory constraints on J0751+1807.)

A 2.1 SOLAR MASS PULSAR MEASURED BY RELATIVISTIC ORBITAL DECAY

DAVID J. NICE AND ERIC M. SPLAVER
Physics Department, Princeton University
Princeton. NJ 08544

arXiv:astro-ph/0508050 v1 1 Aug 2005

$$\dot{P}_b = (-6.4 \pm 0.9) \times 10^{-14}$$

$$\left(\dot{P}_b\right)_{\rm GR} = -\left(\frac{192\pi}{5}\right)\left(\frac{2\pi}{P_b}\right)^{5/3}\left(1+\frac{73}{24}e^2+\frac{37}{96}e^4\right) \times \frac{1}{(1-e^2)^{7/2}} T_\odot^{5/3} \frac{m_1\, m_2}{(m_1+m_2)^{1/3}},$$

$$f_1 \equiv \frac{(m_2 \sin i)^3}{(m_1+m_2)^2} = \frac{x^3}{T_\odot}\left(\frac{2\pi}{P_b}\right)^2$$

Projected semi major axis

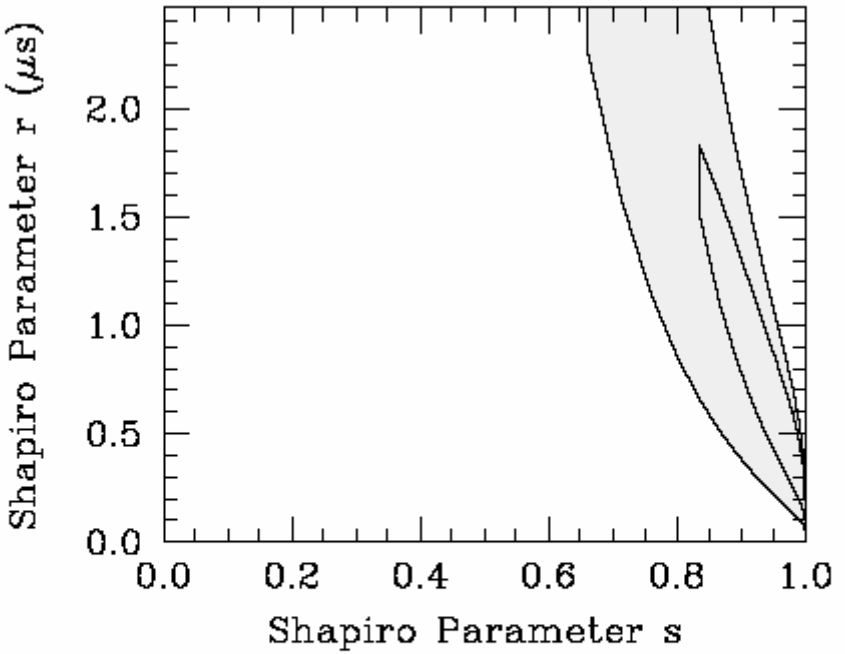

$$\Delta t = -2r \ln\{1 - s \sin[(2\pi/P_b)(t - t_{\rm asc})]\},$$

FIG. 2.— Constraints on Shapiro delay parameters r and s from the basic timing analysis. Inner and outer contours delimit 68% and 95% confidence regions.

TABLE 2
TIMING MODEL PARAMETERS[a]

Basic Timing Model (Three Post-Keplerian Parameters)	
Ecliptic longitude, λ	116°.33362028(2)
Ecliptic latitude, β	−2°.807548(2)
Proper motion in λ, $\mu_\lambda = \cos\beta(d\lambda/dt)$ (mas/yr)	−0.35(3)
Proper motion in β, μ_β (mas/yr)	−6(2)
Parallax (mas), π	1.6(8)
Rotation frequency, ν_0 (s^{-1})	287.457858630106(2)
Rotation frequency derivative, ν_1 (s^{-2})[b]	$-6.4337(4) \times 10^{-16}$
Epoch, t_0 (MJD [TDB])	51800.0
Dispersion measure, DM_0 ($pc\,cm^{-3}$)[c]	30.2489(3)
Dispersion measure derivative, DM_1 ($pc\,cm^{-3}\,yr^{-1}$)	−0.00017(1)
Orbital period, P_b (days)[b]	0.263144266723(5)
Projected semi-major axis, x (lt-s)	0.3966127(6)
Eccentricity, e	$5(11) \times 10^{-7}$
Time of ascending node, t_{asc} (MJD [TDB])	51800.21573411(2)
Orbital period derivative, $\dot{P}_b$ (unitless)	$-6.2(8) \times 10^{-14}$
Shapiro parameters, r and s	see Figure 2
General Relativistic Timing Model (Two Post-Keplerian Parameters)	
Cosine of inclination angle, $\cos i$	$0.41^{+0.11}_{-0.07}$
Pulsar mass, m_1 ($M_\odot$)	2.1(2)
Secondary mass, m_2 ($M_\odot$)	0.191(15)

[a]Figures in parentheses are 68% confidence uncertainties in the last digit quoted.
[b]Observed value, not corrected for acceleration biases; see Table 3.
[c]Formal uncertainty in the timing fit. No attempts were made to correct for pulse shape evolution over frequency.

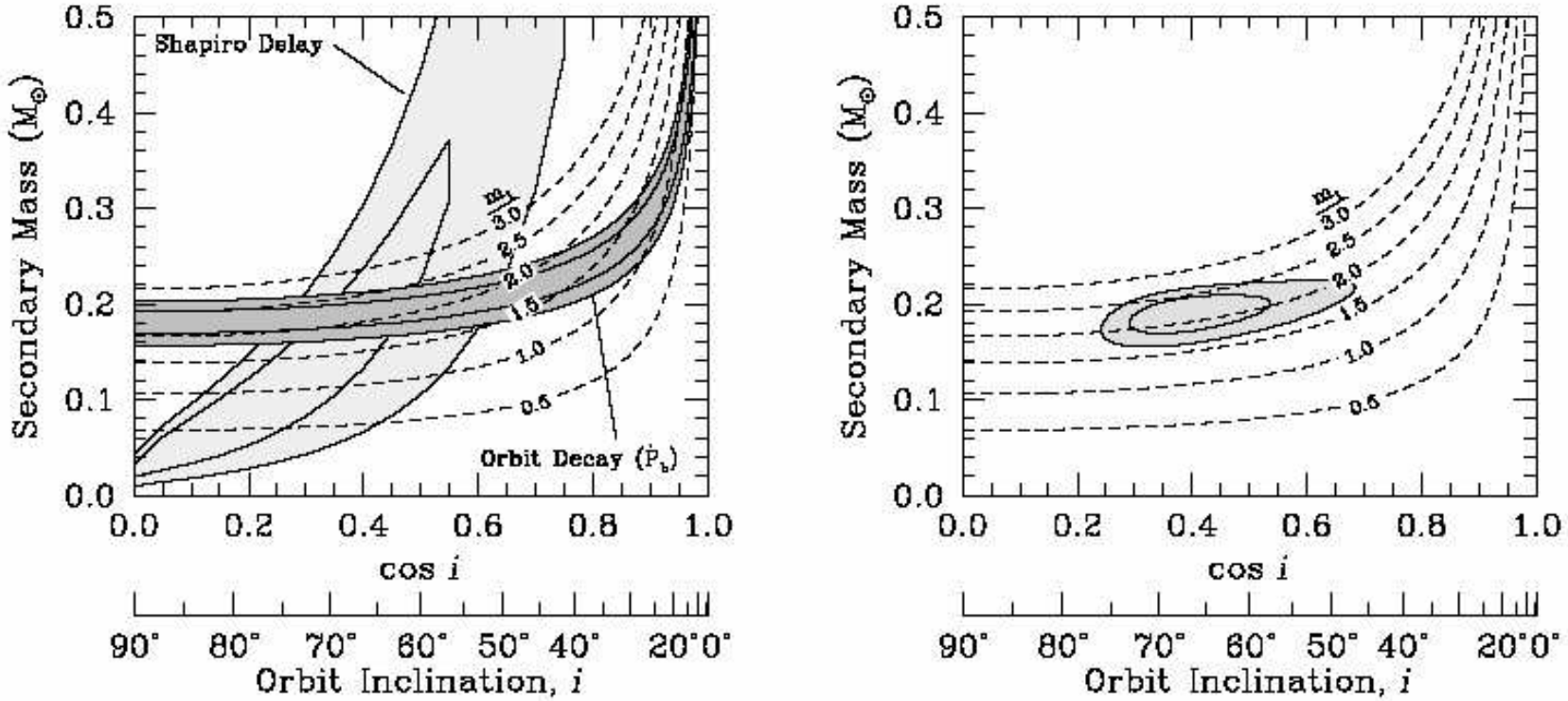

FIG. 3.— Constraints on $\cos i$ and m_2. Dashed lines indicate values of m_1 according to equation 6. (a) *Left plot:* Constraints from the basic timing model, with three post-Keplerian parameters (orbital decay and two Shapiro delay parameters), cast into inclination and mass values via equations 3 through 6. (b) *Right plot:* Constraints from the general relativistic timing model, with two post-Keplerian parameters (inclination and secondary mass). In each plot, inner and outer contours correspond to 68% and 95% confidence limits.

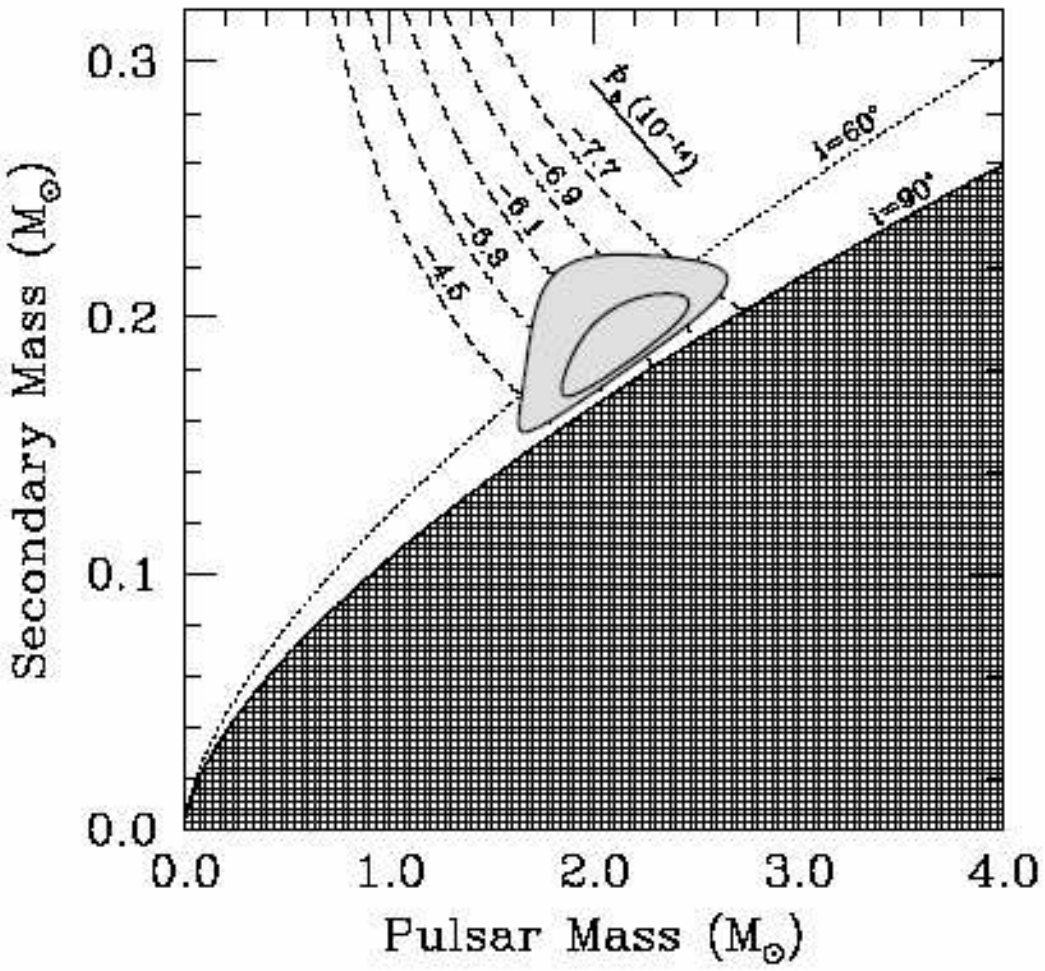

FIG. 4.— Constraints on pulsar and secondary masses from the general relativistic timing model. Confidence limits of 68% and 95% are shown. These are the same constraints as the right plot of figure 3, cast into a different parameterization. The shaded region in the lower left is disallowed by the Keplerian mass function. Dashed lines show constraints from $\dot{P}_b$ alone. A dotted line indicates inclination $i = 60°$.

$$\cos i = \begin{cases} 0.41^{+0.11}_{-0.07} & (68\% \text{ confidence}) \\ 0.41^{+0.27}_{-0.13} & (95\% \text{ confidence}), \end{cases}$$

$$m_1 = \begin{cases} 2.1 \pm 0.2\,\mathrm{M}_\odot & (68\% \text{ confidence}) \\ 2.1^{+0.4}_{-0.5}\ \mathrm{M}_\odot & (95\% \text{ confidence}), \end{cases}$$

and

$$m_2 = \begin{cases} 0.191 \pm 0.015\,\mathrm{M}_\odot & (68\% \text{ confidence}) \\ 0.191^{+0.033}_{-0.029}\ \mathrm{M}_\odot & (95\% \text{ confidence}). \end{cases}$$

cos iは精度はあまりよくならないが、周期の変化は
観測時間の2.5乗で良くなる。

$$\left(\frac{\dot{P}_b}{P_b}\right)_{\rm obs} = \left(\frac{\dot{P}_b}{P_b}\right)_A + \left(\frac{\dot{P}_b}{P_b}\right)_{\dot{G}} + \left(\frac{\dot{P}_b}{P_b}\right)_{\dot{m}} + \left(\frac{\dot{P}_b}{P_b}\right)_Q + \left(\frac{\dot{P}_b}{P_b}\right)_D .$$

TABLE 3
BIASES OF PULSAR AND ORBITAL PERIOD DERIVATIVES

Quantity	$\dot{P}$	$\dot{P}_b$
Measurement ...		
	7.7860×10^{-21}	-6.2×10^{-14}
Uncertainty	$\pm 0.0005 \times 10^{-21}$	$\pm 0.8 \times 10^{-14}$
Acceleration biases ...		
Proper motion	0.35×10^{-21}	0.2×10^{-14}
z-acceleration	-0.19×10^{-21}	-0.1×10^{-14}
Galactic rotation	0.19×10^{-21}	0.1×10^{-14}
Intrinsic value ...		
Measurement−Bias	7.44×10^{-21}	-6.4×10^{-14}
Uncertainty	$\pm 0.4 \times 10^{-21}$	$\pm 0.9 \times 10^{-14}$

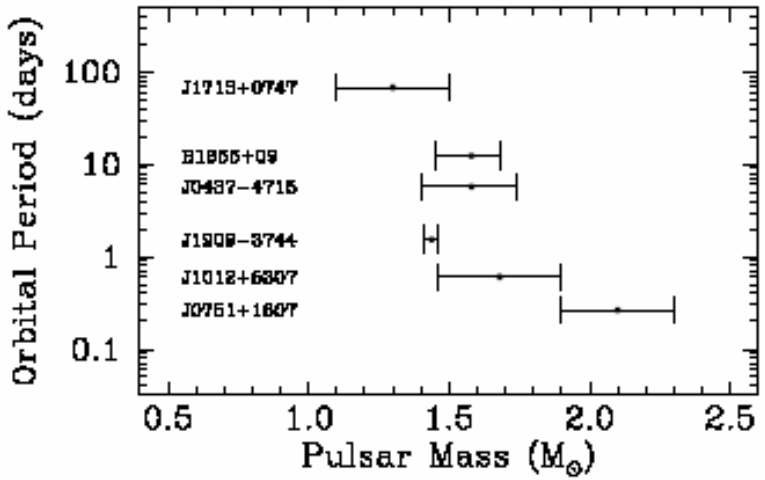

FIG. 5.— Measured pulsar masses in circular pulsar–helium white dwarf binary systems as a function of orbital period. Data are from this paper, Jacoby et al. (2005), Lange et al. (2001), van Straten et al. (2001), and Nice et al. (2005), and references therein.

基礎方程式はQCDの理論

陽子や中性子間に働いて原子核を結合させている強い力はQCD (Quantum Chromo Dynamics)で記述されることが確立している。

Quark F=6

$$L_{QCD} = -\frac{1}{4}F^a_{\mu\nu}F^{a\mu\nu}$$

ゲルマン行列

$$+\sum_{f=1}^{F}\bar{\Psi}_{if}[i\gamma^\mu(\partial_\mu - igA^a_\mu\lambda^a/2)^j_i - m_f\delta^j_i]\Psi_{jf}$$

$$F^a_{\mu\nu} = \partial_\mu A^a_\nu - \partial_\nu A^a_\mu + gf_{abc}A^b_\mu A^c_\nu$$

グルオン場 a=1-8

SU(3)の構造定数

Quark u(up), d(down), s(strange), c(charm), b(bottom), t(top)

Critical point of QCD at finite T and μ, lattice results for physical quark masses

Z. Fodor[a,b], S.D. Katz[a*]

arXiv:hep-lat/0402006 v1 8 Feb 2004

ABSTRACT: A critical point (E) is expected in QCD on the temperature (T) versus baryonic chemical potential (μ) plane. Using a recently proposed lattice method for $\mu \neq 0$ we study dynamical QCD with n_f=2+1 staggered quarks of physical masses on $L_t = 4$ lattices. Our result for the critical point is $T_E = 162 \pm 2$ MeV and $\mu_E = 360 \pm 40$ MeV. For the critical temperature at $\mu = 0$ we obtained $T_c = 164 \pm 2$ MeV. This work extends our previous study [Z. Fodor and S.D.Katz, JHEP 0203 (2002) 014] by two means. It decreases the light quark masses ($m_{u,d}$) by a factor of three down to their physical values. Furthermore, in order to approach the thermodynamical limit we increase our largest volume by a factor of three. As expected, decreasing $m_{u,d}$ decreased μ_E. Note, that the continuum extrapolation is still missing

$m_{u,d} = 0.0092$ and $m_s = 0.25$ $12^3 \cdot 24$ lattices.

values. The pion to rho mass ratio, extrapolated to our $T \neq 0$ parameters, is 0.188(2) (its physical value is 0.179), whereas the pion to K mass ratio in the same limit is 0.267(1) (its physical value is 0.277).

The partition function of lattice QCD the link variables U

$$Z(\beta, m, \mu) = \int \mathcal{D}U \exp[-S_b(\beta, U)][\det M(m, \mu, U)]^{n_f/4}$$

$$= \int \mathcal{D}U \exp[-S_b(\beta_w, U)][\det M(m_w, \mu_w, U)]^{n_f/4}$$

$$\left\{\exp[-S_b(\beta, U) + S_b(\beta_w, U)] \left[\frac{\det M(m, \mu, U)}{\det M(m_w, \mu_w, U)}\right]^{n_f/4}\right\},$$

μ is the quark chemical potential n_f degenerate staggered quarks the determinant of the quark matrix M the bosonic action S_b

$$p = kT \ln Z/V$$

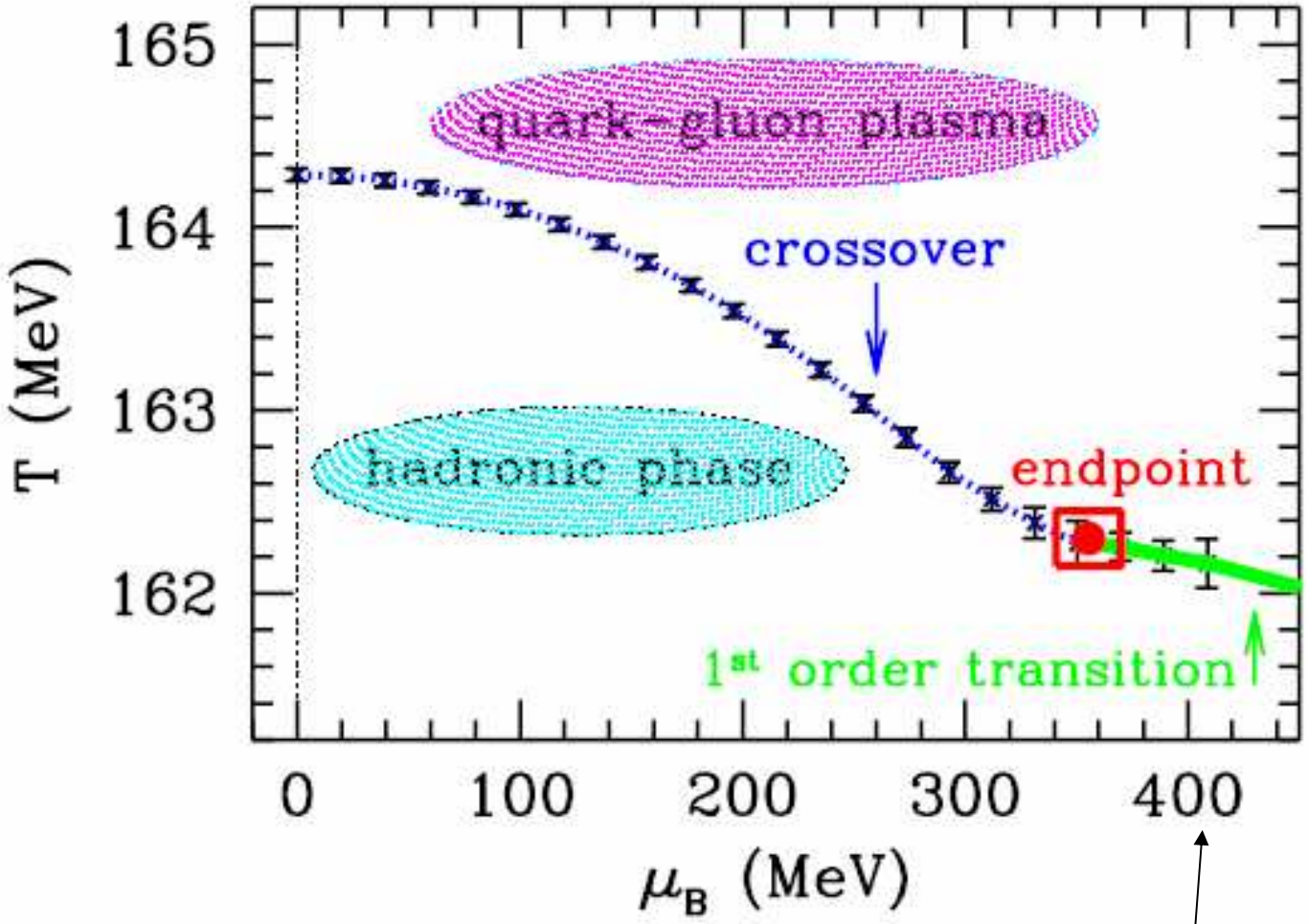

Figure 2: The phase diagram in physical units. Dotted line illustrates the crossover, solid line the first order phase transition. The small square shows the endpoint. The depicted errors originate from the reweighting procedure. Note, that an overall additional error of 1.3% comes from the error of the scale determination at T=0. Combining the two sources of uncertainties one obtains $T_E = 162 \pm 2$ MeV and $\mu_E = 360 \pm 40$ MeV.

このあたりが核密度

2つの問題

1） 格子の数が少ない。⇒数値物理の初期には必ずそうなる
問題なし。

2） 温度が低いときの計算法が確立していない
⇒数値物理の初期には必ずそうなる
問題なし。1発のアイデアで解決
する場合を数々見てきた。

例1） 数値相対論　初期は28X28、計算の不安定性は
Conformal TT Decompositionで解決
例2） Newton　N体問題
Multi-time step法、Tree法、Grape等の専用計算機

状態方程式を重力波から得る

中性子星の状態方程式

G=c=1の単位系

$$ds^2 = e^{\nu(r)}dt^2 - \frac{dr^2}{(1-\frac{2m(r)}{r})} - r^2(d\theta^2 + \sin\theta^2 d\phi^2)$$

$$\frac{dm(r)}{dr} = 4\pi r^2 \rho(r)$$

$$\frac{d\nu(r)}{2dr} = \frac{m(r)+4\pi r^3 p(r)}{r^2(1-2m(r)/r)}$$

連星中性子星の軌道の変化

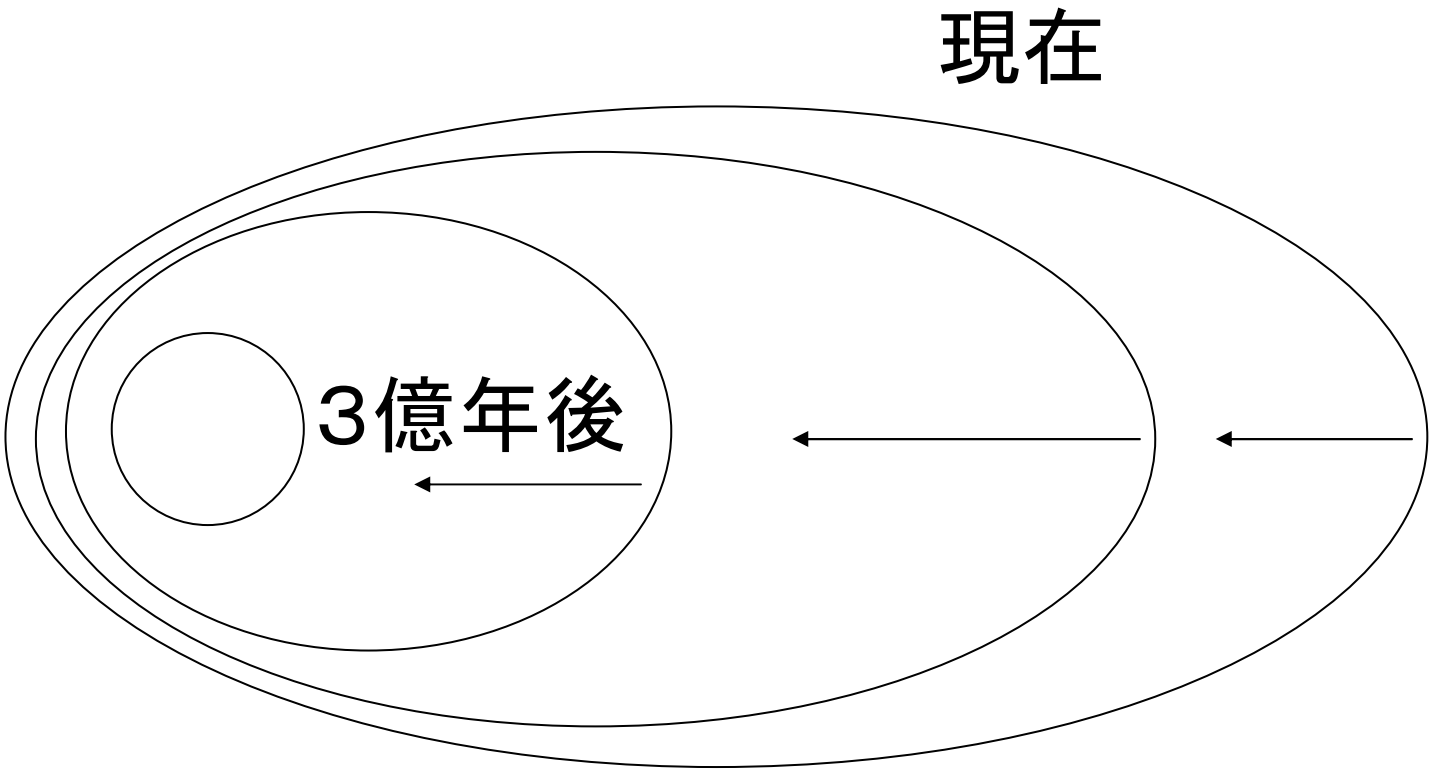

最後の3分間

- チャープ信号
- ブラックホール

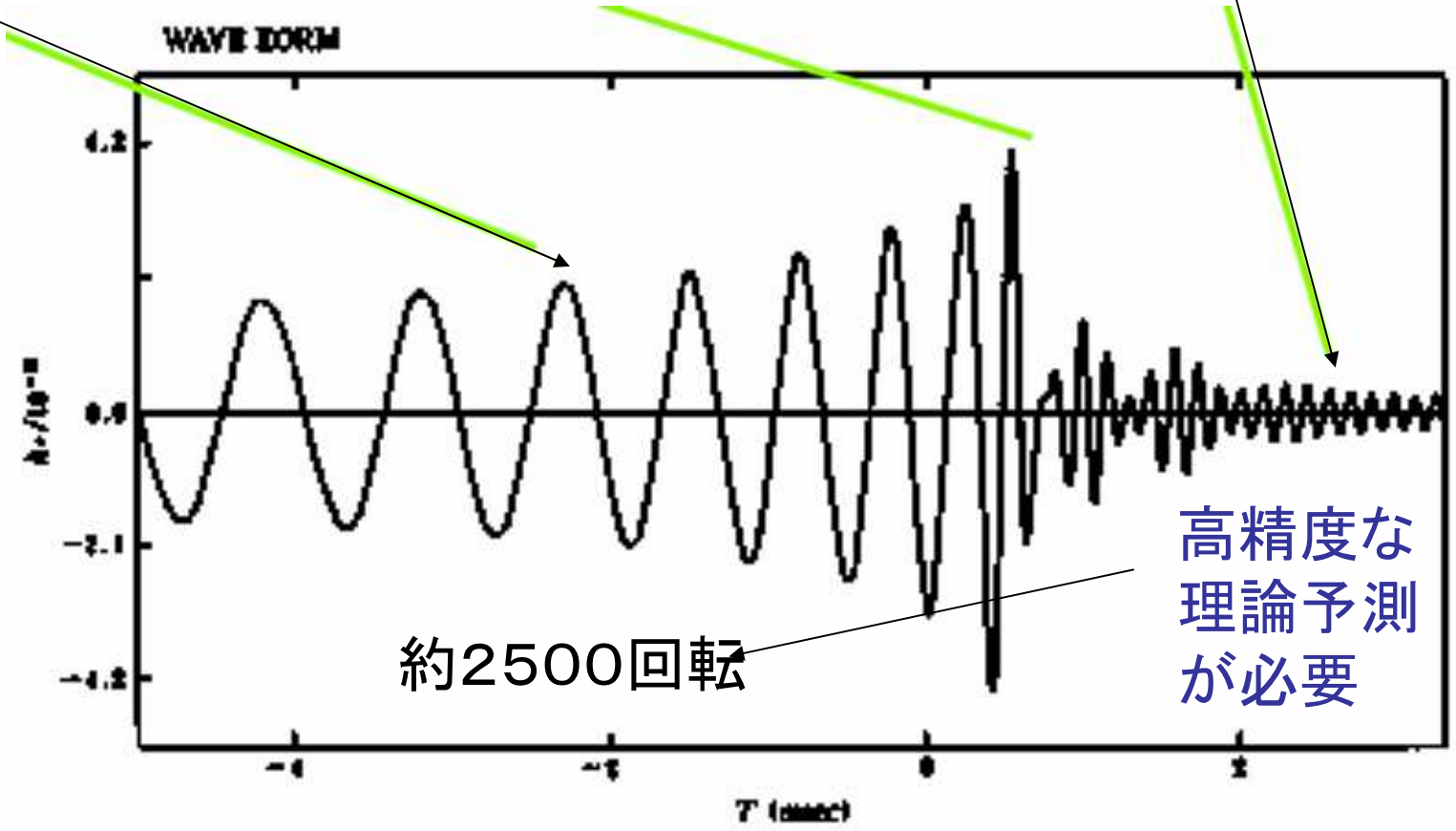

重力波
の振幅

- 20Hz kHz
- ← 3分間 →

連星中性子星の合体のシミュレーション（密度）

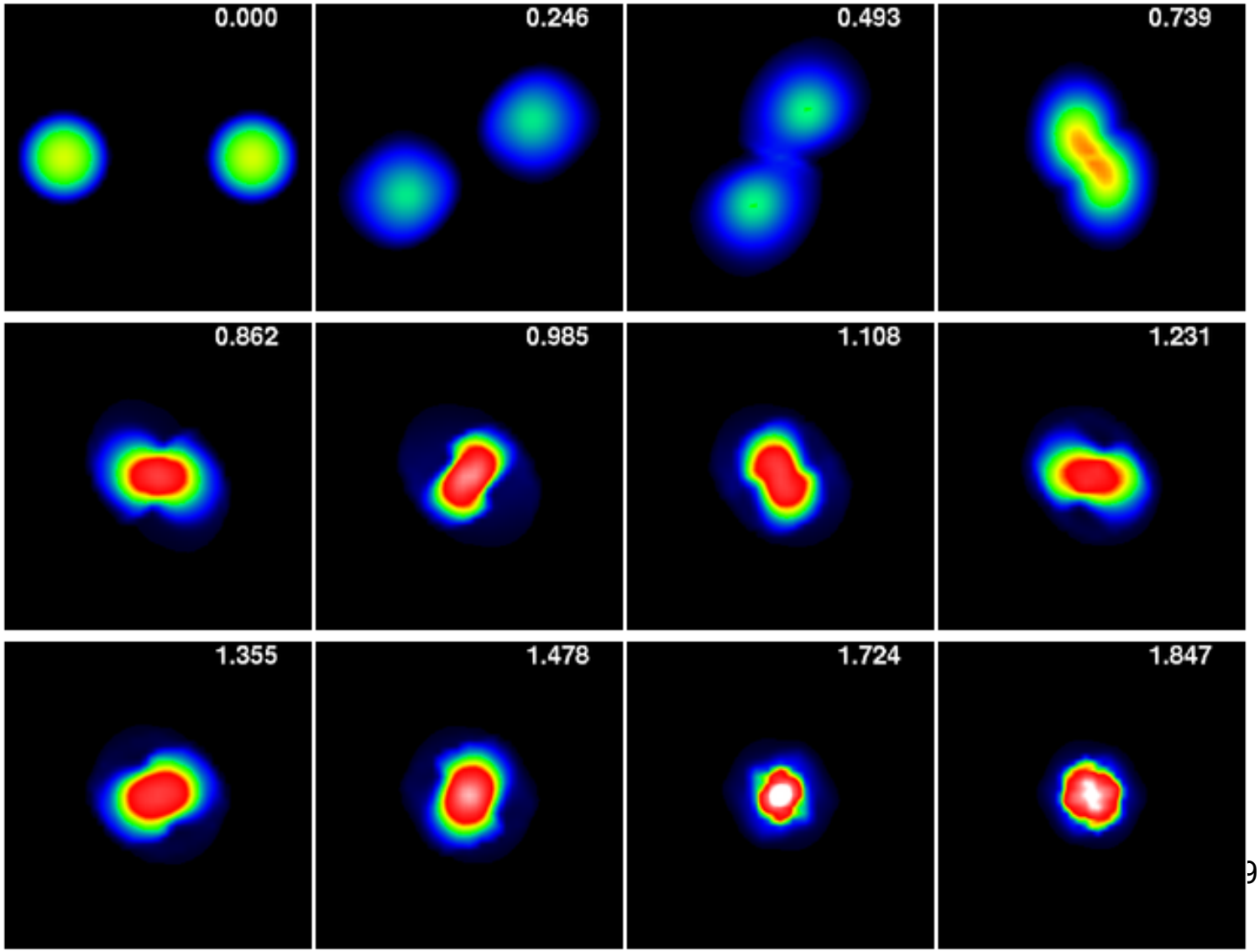

TOV方程式(1939)

- 一般相対論的平衡解(Tolman Oppenheimer Volkov 方程式)

$$\frac{dp}{dr} = -\rho \frac{Gm}{r^2} f$$

$$f = (1 + \frac{4\pi r^3 p}{mc^2})(1 + \frac{p}{\rho c^2})(1 - \frac{2Gm}{rc^2})^{-1}$$

$$p = p(\rho)?$$

逆問題

中心密度と状態方程式を与えると、中性子星の半径と質量は
TOV方程式を中心から解くことによって決まる。

中性子星の半径が質量の関数として得られたら状態方程式は
求まるか？

YES.　Lindblom 1992

THE ASTROPHYSICAL JOURNAL, 398:569–573, 1992 October 20

DETERMINING THE NUCLEAR EQUATION OF STATE FROM NEUTRON-STAR MASSES AND RADII

LEE LINDBLOM

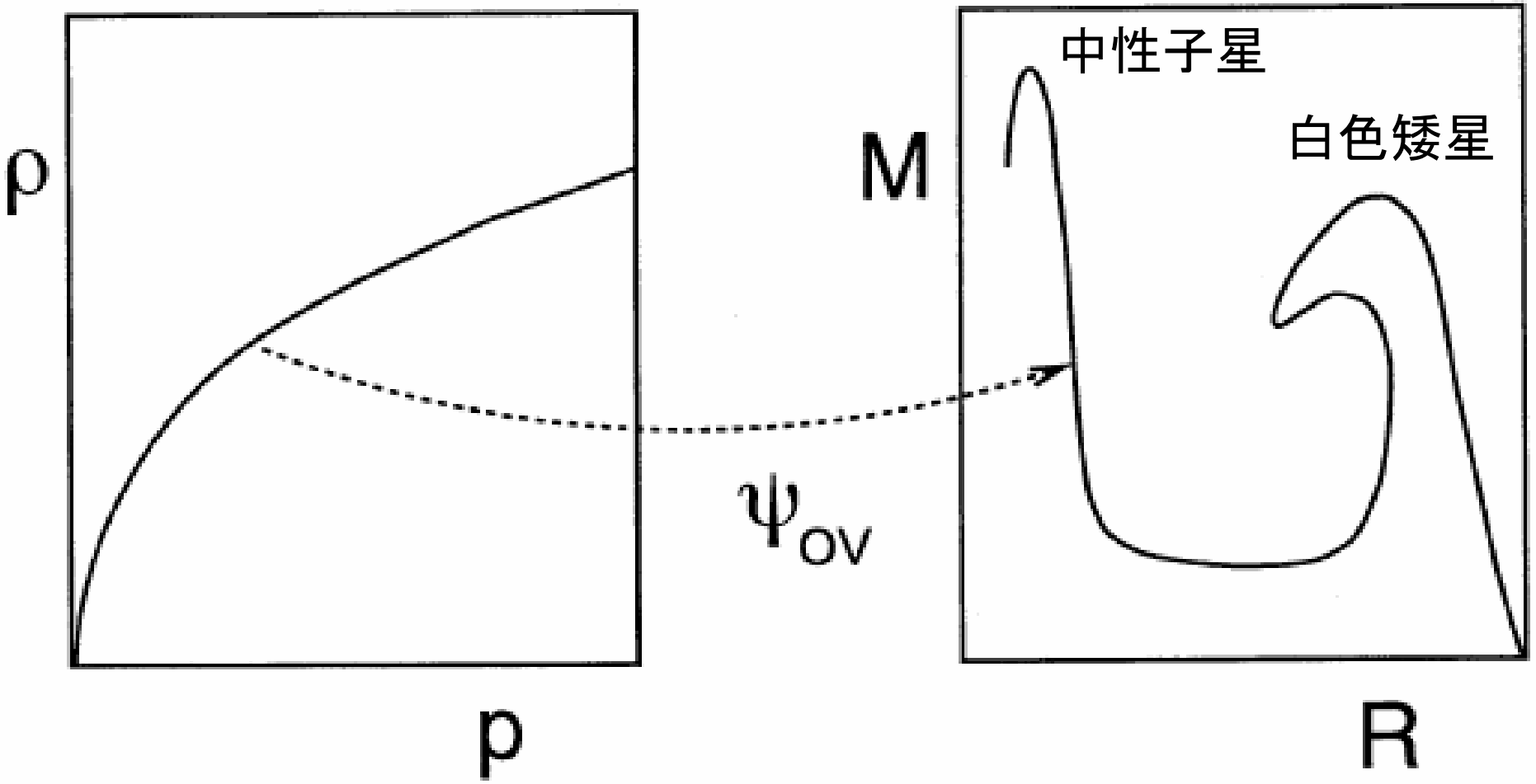

FIG. 1.—A schematic representation of the map—generated by the OV equations—that takes equations of state into mass-radius relationships.

エンタルピー h

$$h(p) = \int_0^p \frac{d\acute{p}}{\rho(\acute{p}) + \acute{p}}$$

TOV方程式

$$\frac{dm}{dh} = -\frac{4\pi\rho(h)r^3(r-2m)}{m + 4\pi r^3 p(h)} \qquad \frac{dr}{dh} = -\frac{r(r-2m)}{m + 4\pi r^3 p(h)}$$

1) $p(h), \rho(h)$ are known for $h < h_i$

2) $M = M_i, R = R_i$

for $p_c = p(h_i) = p_i, \rho_c = \rho(h_i) = \rho_i$

3) for M_{i+1}, R_{i+1} integrate TOV

from $h = 0$ to $h = h_i$

4) $m = m_i, r = r_i$

$$\rho_c = \rho_i + \frac{5}{2}\left(\frac{3m_i}{4\pi r_i^3} - \rho_i\right)$$

$$p_c = p_i + \frac{2\pi}{3}(\rho_i + p_i)(\rho_i + 3p_i)r_i^2\left[1 + \frac{2\pi}{3}(4\rho_i + 3p_i)r_i^2\right] + \frac{\pi}{3}(6\rho_i + 11p_i)\left(\frac{3m_i}{4\pi r_i^3} - \rho_i\right)r_i^2$$

$$h_c = h_i + \frac{p_c - p_i}{2(\rho_i + p_i)}\left(3 - \frac{\rho_c + p_c}{\rho_i + p_i}\right)$$

We can extend the equation of the state up to

$$h = h_c = h_{i+1}$$

問題点　たくさんの質量と半径のデータがいるが、それは可能か？

M,Rが1個しか得られない場合

$\rho = \rho_i$　では状態方程式が判っているとする

$$\frac{p}{p_i} = \left(\frac{\rho}{\rho_i}\right)^{\log (p_c/p_i)/\log (\rho_c/\rho_i)} .$$

と仮定

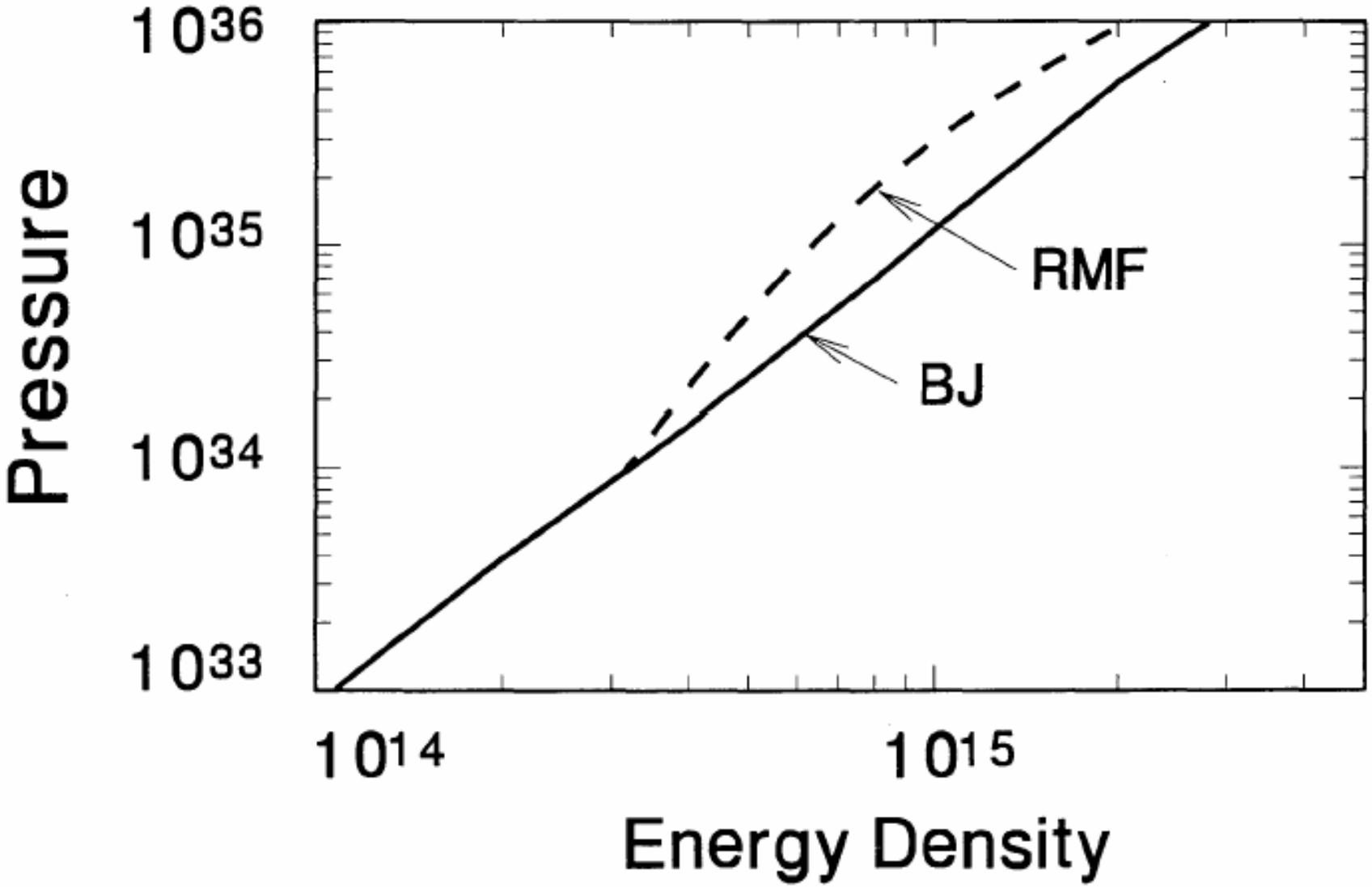

FIG. 2.—The equations of state used to study the inversion of the OV map: BJ is the Bethe & Johnson (1974) equation of state (model 1); and RMF is the relativistic-mean-field equation of state of Serot (1979).

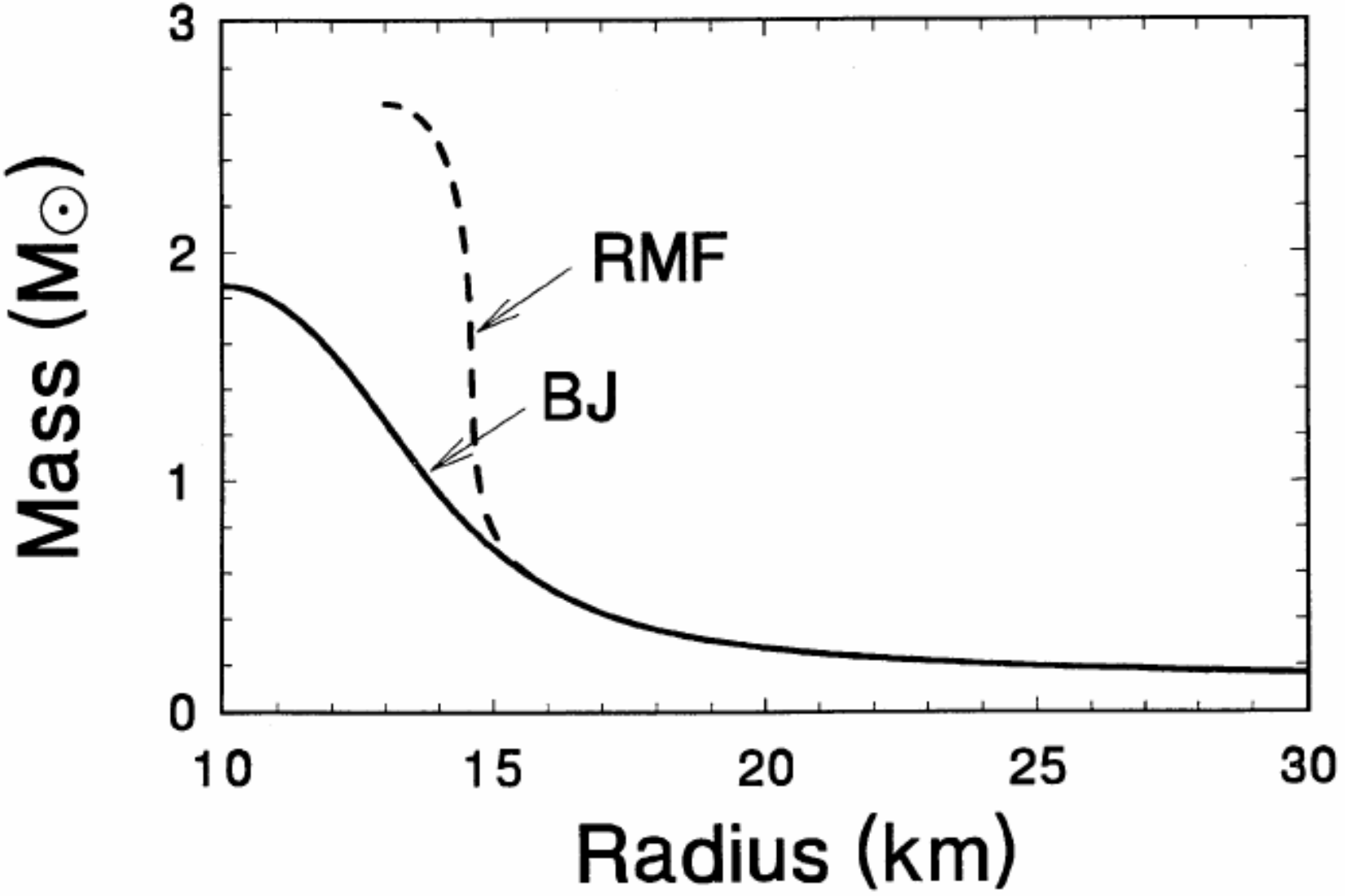

FIG. 3.—The mass-radius relationships determined by the OV equations from the BJ and the RMF equations of state.

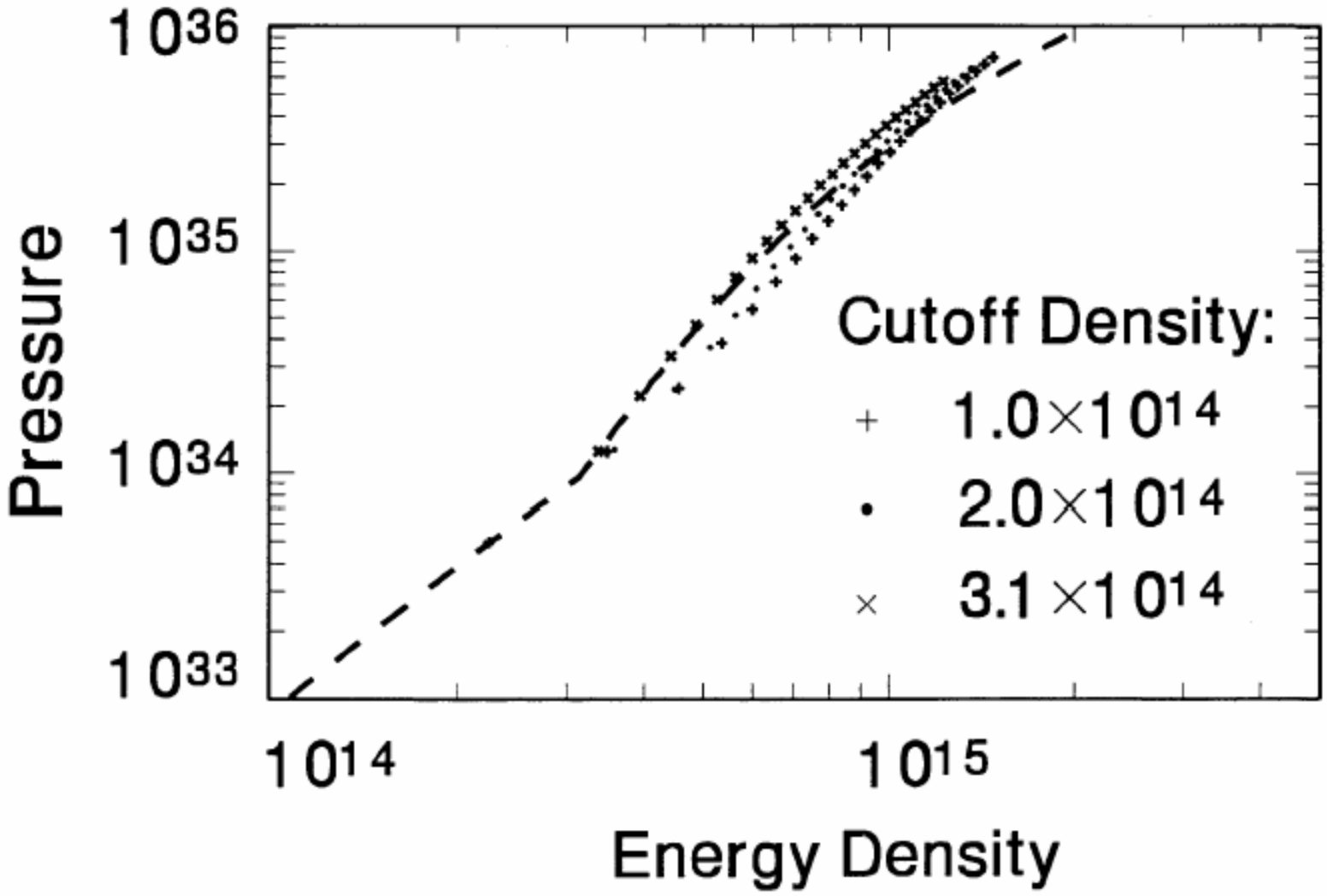

FIG. 4.—The equation of state inferred from the RMF mass-radius data using the "one-step" algorithm. Each equation-of-state point is determined from a single neutron star mass and radius, and a knowledge of the equation of state below the specified cutoff density. For comparison the original RMF equation of state is plotted as the dashed curve.

如何にして中性子星の質量と半径を決定するか？

質量は連星中性子星とブラックホールのチャープシグナルから決定できる？

1） 重力波のpower spectrum にform factorとして半径の逆数に比例した振動数の間隔でピークが表れる
Saijo and Nakamura 2001

$$\Delta\nu = 5\mathrm{kHz}\left(\frac{R}{10\mathrm{km}}\right)^{-1}$$

状態方程式に依存しないが、振動数は高い

VOLUME 85, NUMBER 13 PHYSICAL REVIEW LETTERS 25 SEPTEMBER 2000

Possible Direct Method to Determine the Radius of a Star from the Spectrum of Gravitational Wave Signals

Motoyuki Saijo*
Department of Physics, Waseda University, 3-4-1 Okubo, Shinjuku, Tokyo 169-8555, Japan
Takashi Nakamura†

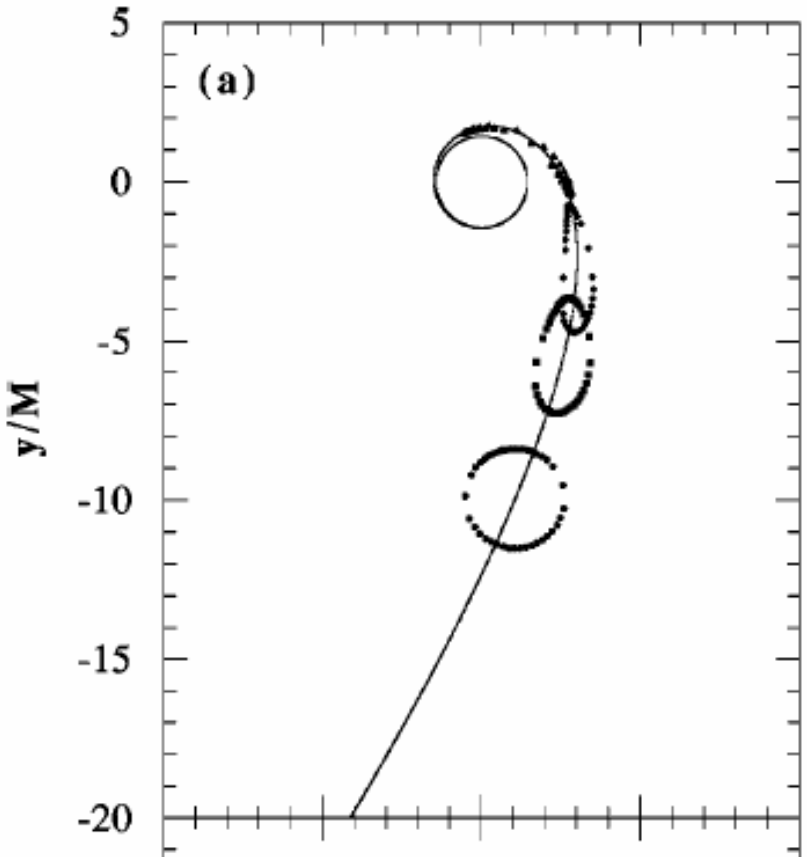

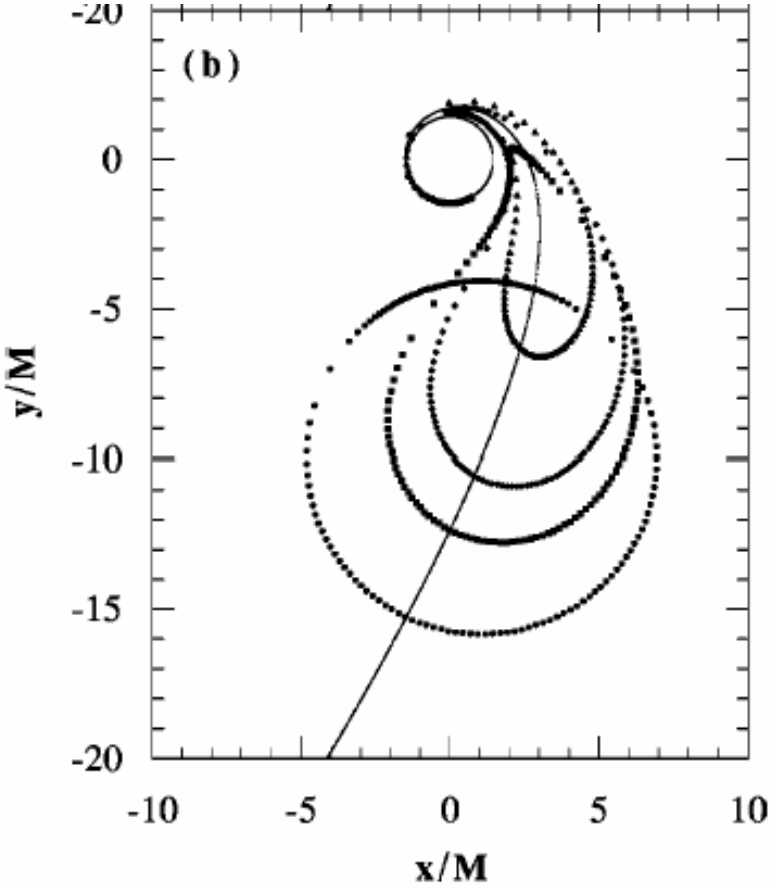

FIG. 19. Deformation of the shape of the spherical disk whose radius is set up at $r=10M$ in the case of $a/M=0.9$, $\tilde{L}_z/M=2$ [(a) $R/M=1.56$, (b) $R/M=5.88$]. Solid line shows the geodesic for the center of gravity of the disk, while circle, square, diamond, and triangle show the edge of the disk where the location of the center is at $r=10M$, $6M$, $4M$, $2M$, respectively.

物の大きさを知るには
何かを当てるか破壊する。

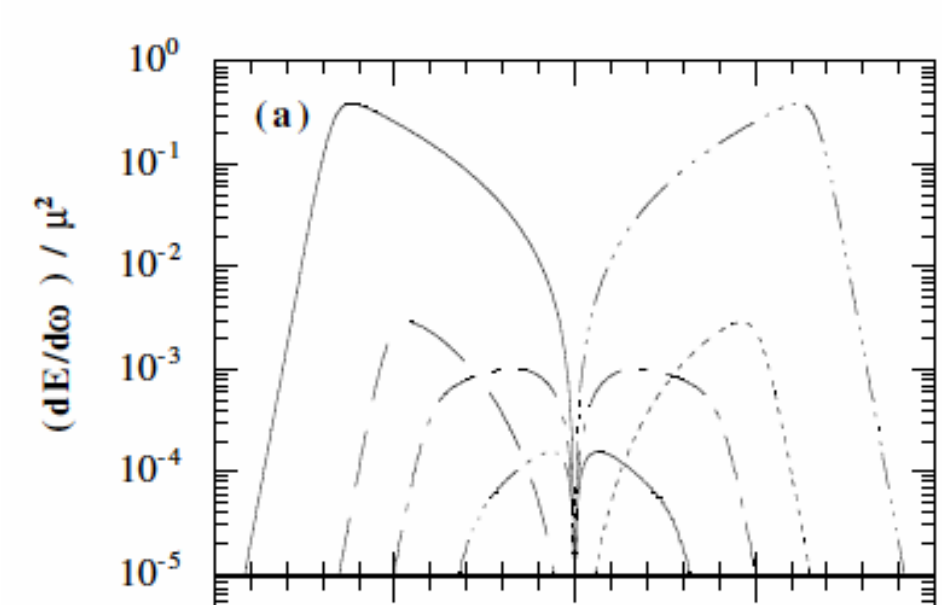

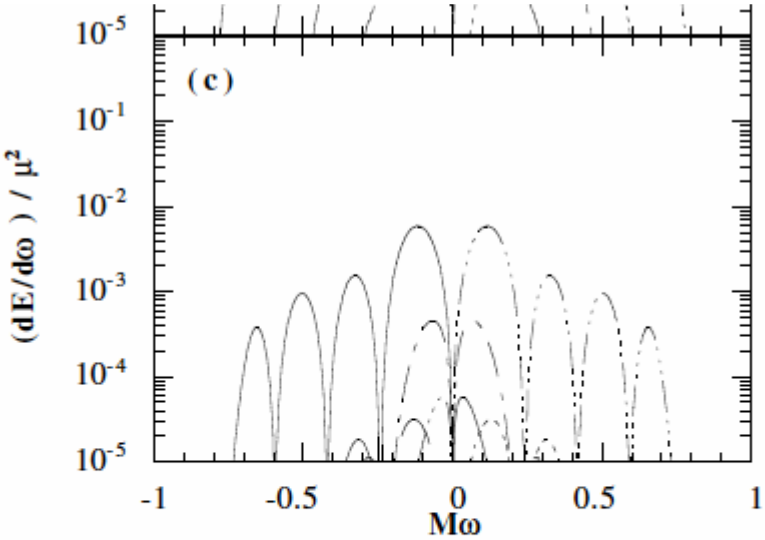

FIG. 1. Energy spectrum of gravitational waves from a dust disk star moving on an equatorial plane in Kerr spacetime whose radius is set up at $r_0 = 10M$ for the case of $a/M = 0.9$, $\tilde{L}_z/M = 2$ [(a) $R/M = 0$ (test particle), (b) $R/M = 1.56$, (c) $R/M = 5.88$]. We show only the $l = 2$ mode. Solid, dashed, dash-dotted, dotted, and dash-three-dotted lines denote the cases of $m = -2$, -1, 0, 1, 2, respectively.

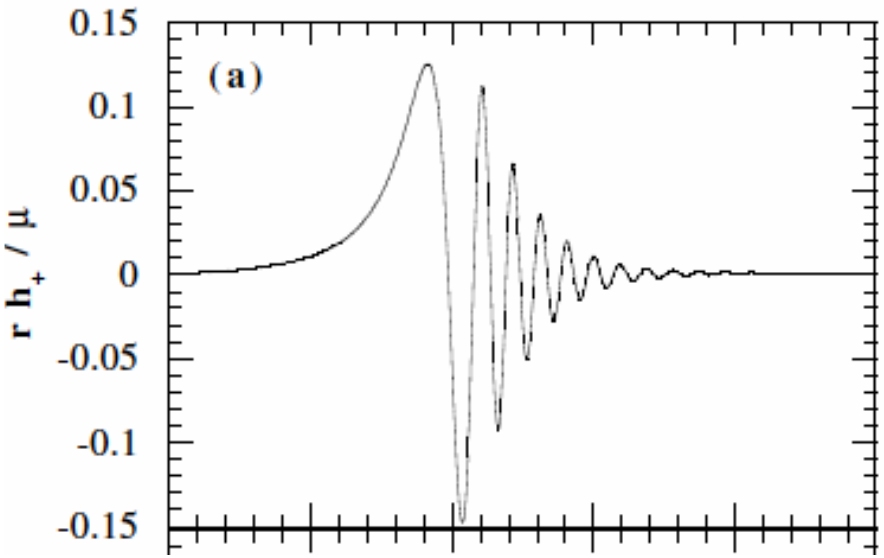

構造を持たない点粒子

構造を持つ場合

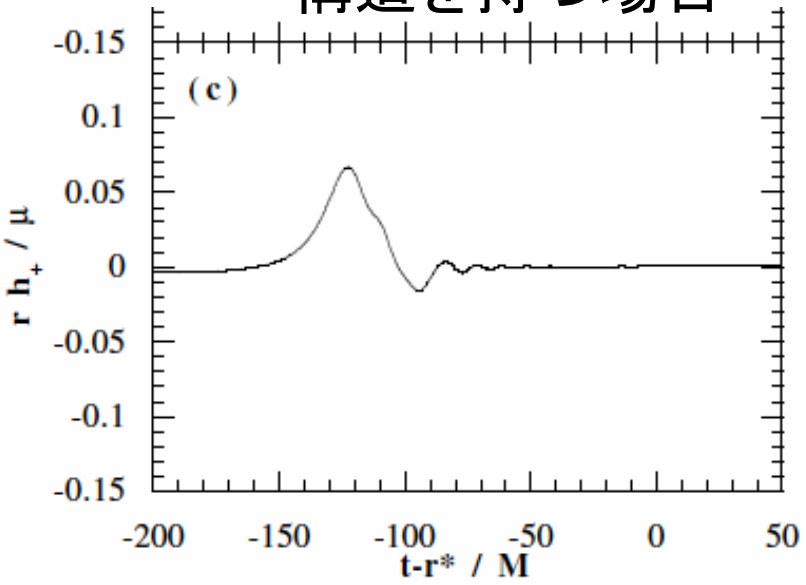

$$A^{(\mathrm{disk})}_{lm\omega} = f_{m\omega} A^{(\mathrm{particle})}_{lm\omega},$$

$$f_{m\omega} = 2\frac{\mu}{S}\int_{r_0-R}^{r_0+R} dr\, r\, \frac{\sin[m\phi_0(r)]}{m} \times e^{i\{\omega[T(r)-T(r_0)]-m[\Phi(r)-\Phi(r_0)]\}},$$

$$\phi_0(r) = \cos^{-1}\frac{r^2 + r_0^2 - R^2}{2rr_0},$$

$$S = 2\int_{r_0-R}^{r_0+R} dr\, r\,\phi_0(r).$$

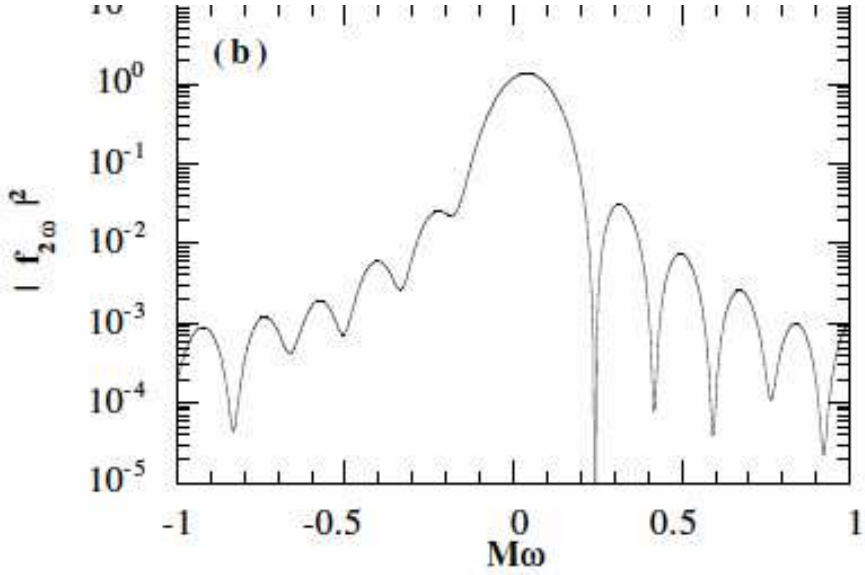

FIG. 3. Form factor of the dust disk star moving on an equatorial plane in Kerr spacetime whose radius is set up at $r_0 = 10M$ for the case of $a/M = 0.9$, $\tilde{L}_z/M = 2$ [(a) $R/M = 1.56$, (b) $R/M = 5.88$]. We show only the $l = m = 2$ mode, because $m = 2$ is a dominant mode for the above parameters in $l = 2$. It is clear that the form factor is responsible for the spectra in Fig. 1.

$f_{m\omega}$ and $A^{(\mathrm{particle})}_{lm\omega}$ are a form factor and the amplitude of gravitational waves at infinity for a single particle

$$M < 4.64 M_\odot \left(\frac{1.4M_\odot}{M_s}\right)^{1/2}\left(\frac{R}{10\ \mathrm{km}}\right)^{3/2}\left(\frac{6M}{r_c}\right)^{3/2},$$

TABLE I. Comparison with the characteristic length from the energy spectrum of gravitational waves to the radius of the disk. R denotes the coordinate radius.

R/M	$\Delta\omega$	$1/\Delta\omega$
3.09	0.335	2.99
3.83	0.270	3.70
4.54	0.233	4.29
5.22	0.200	5.00
5.88	0.175	5.71

２） ISCO（Inner Most Stable Orbit) での重力波の振動数が決定可能とする。 つまり、ISCO以内では急速に重力波の振幅が下がると考える。

ISCOは連星の各質量と状態方程式に依存する。
⇒半径、質量と同様のプログラムが可能？

一般相対論での
ケプラー問題

円軌道の角運動量
依存性

重力波放出で
角運動量が減少
⇒円軌道の半径が減少
⇒重力波の振動数増大

最小円軌道の後は
ほぼ自由落下

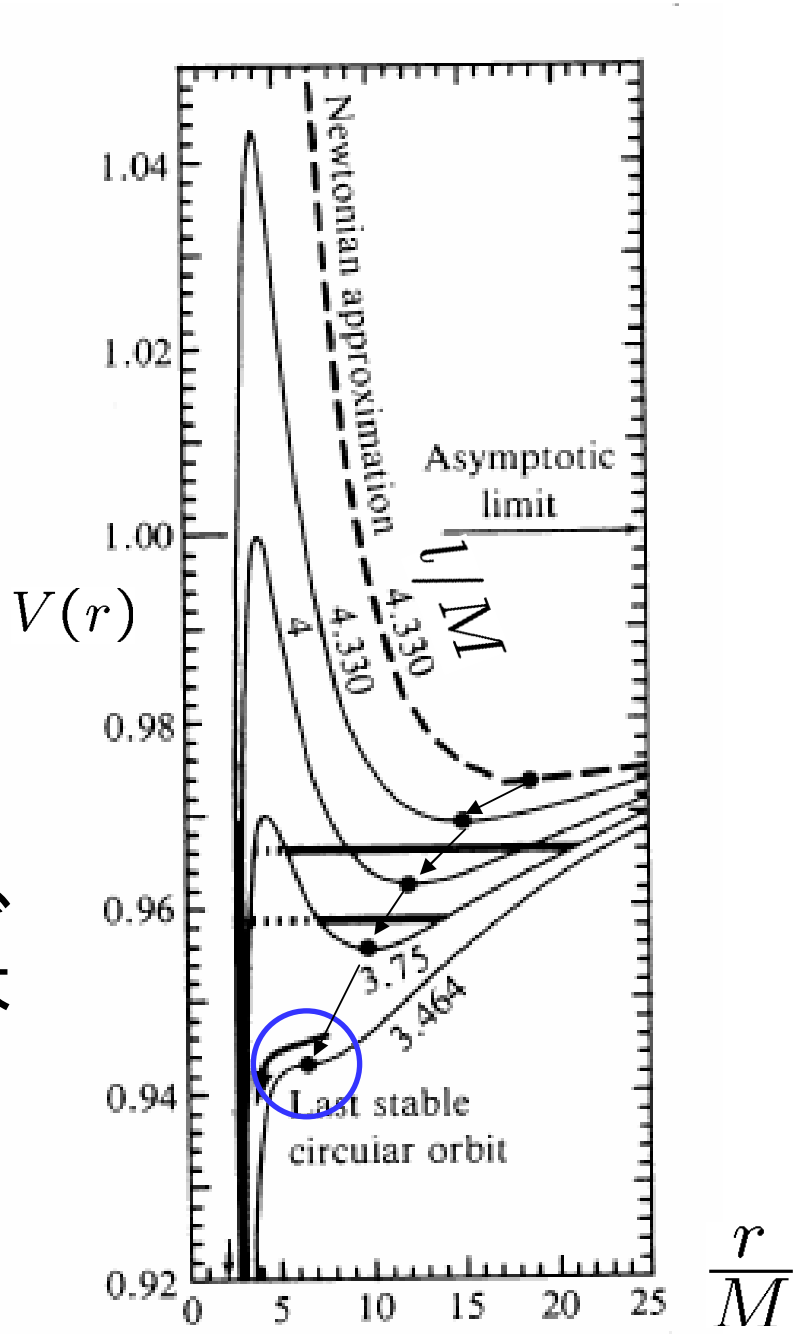

中性子星の状態方程式は全く不明？？？

１）QCDにもとずいた計算が完成するのを待つか？

２）重力波を使って質量と半径の関係を決めて
　　逆問題を解くか？

３）両者が同時進行するのがベスト！！